SLAC-82

UC-32, Mathematics and Computers
UC-34, Physics
UC-37, Instruments

THE HUMMINGBIRD FILM DIGITIZER SYSTEM

by

J. van der Lans, J.-L. Pellegrin, H. J. Slettenhaar*

Technical Report
Prepared Under
Contract AT(04-3)-515
for the USAEC
San Francisco Operations Office

Printed in USA. Available from CFSTI, National Bureau of Standards,
U.S. Department of Commerce, Springfield, Virginia 22151
Price: Printed Copy $3.00; Microfiche $0.65

* While on leave from CERN, Geneva, Switzerland.

ACKNOWLEDGMENTS

The authors wish to stress that the successful completion of the construction phase of this project has been an effort to which numerous individuals have contributed. Our thanks are due to our highly skilled technicians, G. Szongott, V. Smith and V. Hamilton, who have participated in the actual construction. Dr. J. L. Brown has given us his invaluable aid, particularly in the areas of accuracy evaluation and the design of the calibration procedures that make these devices useful for the purposes for which they were intended. We also wish to thank the programming staff of the Automatic Data Analysis Group, particularly A. Leino for the many diagnostic programs that have been essential in the debugging of the hardware. Greatly appreciated is the continuous support and encouragement we received from Prof. W. F. Miller and his suggestions towards the use of this kind of equipment in other areas of graphic data processing.

TABLE OF CONTENTS

LIST OF FIGURES

INTRODUCTION

The devices described find, among others, application in the automatic analysis of film generated in high energy nuclear physics experiments. These films are mainly of two kinds.

Spark Chamber Film. A spark chamber is a nuclear particle detector consisting of several parallel metal plates. The space between the plates is filled with a neon-helium gas mixture. After a traversing particle has been detected a short high voltage pulse is applied which gives rise to sparks between the plates in the regions where the gas has been locally ionized by the passing charged particle. A photograph is taken, recording the particle trajectory. The spark images appear as small dark areas on the transparent film. Figure 1(a) shows the basic principle of operation and a typical photograph produced.

Bubble Chamber Film. A bubble chamber is basically a container filled with, for instance, liquid hydrogen. Shortly before a beam of nuclear particles arrives a piston or bellows suddenly enlarges the volume of the chamber. The hydrogen then becomes superheated. Particles passing through the vapor cause boiling, thus leaving a track of bubbles, which when photographed record the particle trajectories. Individual bubbles appear on the film as dark dots with an approximate diameter of one mil. In Fig. 1(b) the principle is explained and an example shown.

Several systems for the automatic analysis of film generated in high energy nuclear physics experiments have been devised and are in varying degrees of operation. All of these systems operate on-line to computers, which range in size from as small as a DEC PDP 4 for data taking and device control to as large as a CDC 6600 for complete on-line analysis.[1] The devices which are the subject of this report have been designed at the Stanford Linear Accelerator Center over the past two years and operate on-line to an IBM 360/75. The entire system consists of two programmable film scanners and a computer-controlled display with lightpen. Figure 2 is a block diagram showing the system components and their connection to the 360/75. The film-scanning devices have been designed primarily for the accurate digitization of spark and bubble chamber film. On these films the data to be digitized is in the form of small opaque areas on transparent film. The size of these spark or bubble images on the film is typically from 20 to 50 μm. Only the center coordinates of these opacities, as determined

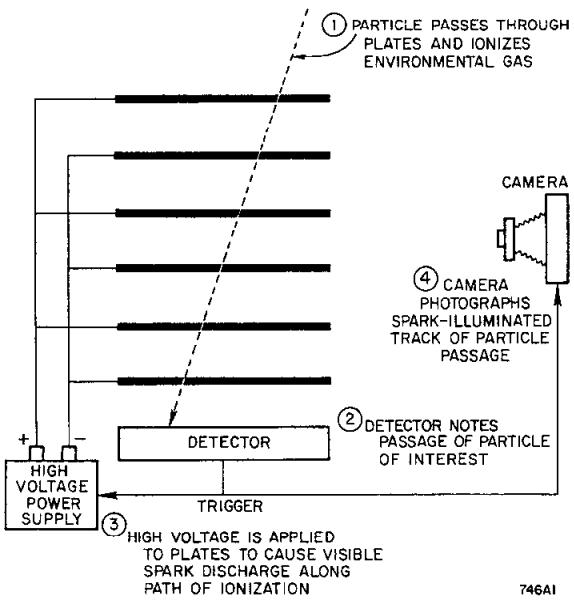

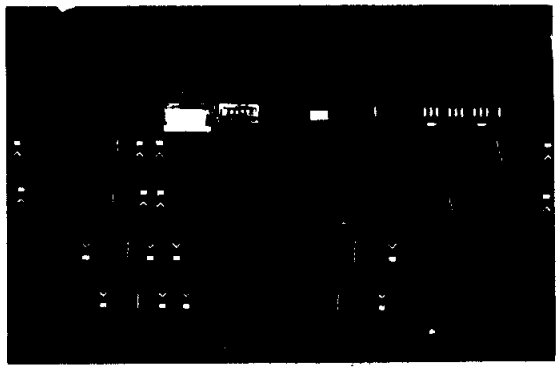

FIG. 1a--Spark chamber principle.

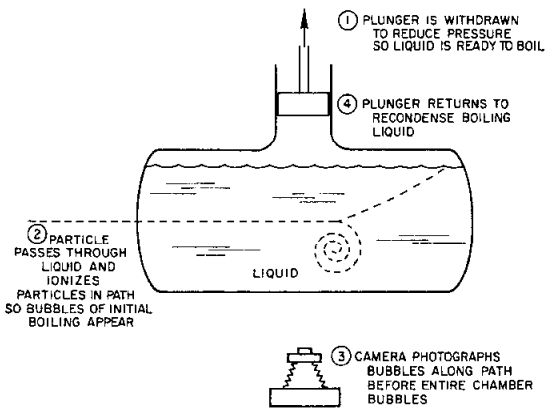

FIG. 1b--Bubble chamber principle.

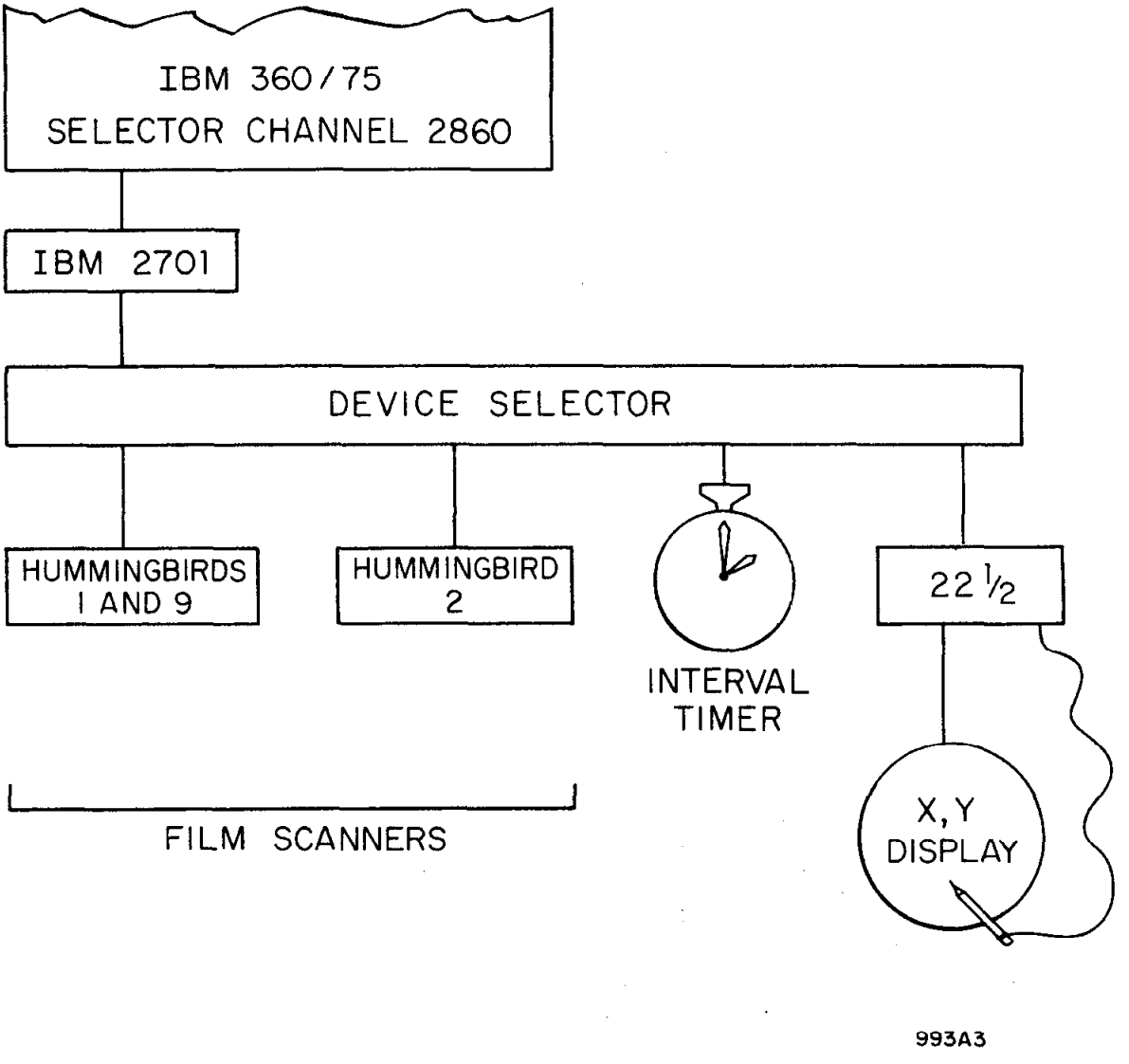

FIG. 2--System block diagram.

by circuitry, are transmitted to the computer. In order to permit research in other areas of graphic data processing, one of the scanners may operate in a sampling mode in which light samples are taken across a scanline, digitized and transmitted with the coordinates of incidence.

This report is a compilation of internal technical descriptions and parts of previously published material. It consists of two main parts, the first one of which contains some of the design considerations and a description of their implementation. The second part describes in detail the problems and the solution to the problems involved in the usage of cathode ray tubes in high resolution, high precision measuring applications. A description of the digital logic for the controlling functions, interpretation and execution of the orders sent by the computer, transmission and receiving of data, the accurate digitization of the film data as well as the computer-driven display device which forms an integral part of this graphical data processing system are the subject of internal technical notes mentioned in the list of references.

I. SYSTEM CONSIDERATIONS AND GENERAL DESCRIPTION

The spot on the face of a cathode ray tube is deflected in a TV-raster scan mode. The film is accessed in one or a number of, program specified, randomly located rectangles. The density of scanlines, a threshold setting on the photomultiplier signal and the scanline orientation along or perpendicular to the length of the film are under program control. The pattern on the face of the tube is imaged onto the film, while the light passing through the film is collected and focused onto the cathode of a photomultiplier. The presence of dark areas on an otherwise transparent film is sensed by the photomultiplier upon which its center is digitized and subsequently transmitted to the computer. Figure 3 shows the different parts of the film reader and their interaction.

The early flying spot digitizers that have found application in the analysis of nuclear physics film were mechanical. A moving spot of light is generated by crossing two fine slits, one of which is held stationary, while the other is on a rotating disk behind which a light source is located. The moving spot is focused on the film, which in turn is moved past the scanning spot.[1] Although a very high resolution and precision may be obtained in this manner, an installation of this kind is generally large and expensive and requires a great deal of maintenance.

The usage of cathode ray tubes as the spot generator in flying spot digitizers seems more advantageous from the point of view of flexibility, cost and maintenance; however, several inherent CRT-drawbacks have to be eliminated before one may attempt to use these devices in applications where high resolution and precision are of importance. The on-line to a computer aspect of the described scanning equipment facilitates the usage of CRT's for this application.

A high resolution cathode ray tube has a flat-face plate for (optical) depth of field reasons. This produces two effects. The so-called pincushion distortion is caused by the fact that the deflection distance on the flat face is not linearly proportional to the current in the deflection coils. A certain amount of linearization (usually to about 0.5%) may be obtained by either circuitry or the attachment of permanent or electromagnets to the tube. Better linearization by hardware means is impractical and the residual distortion is removed by calibration. Since computer calibration cannot be avoided, no hardware correction at all is implemented in the hummingbird devices. It has been shown that the differential

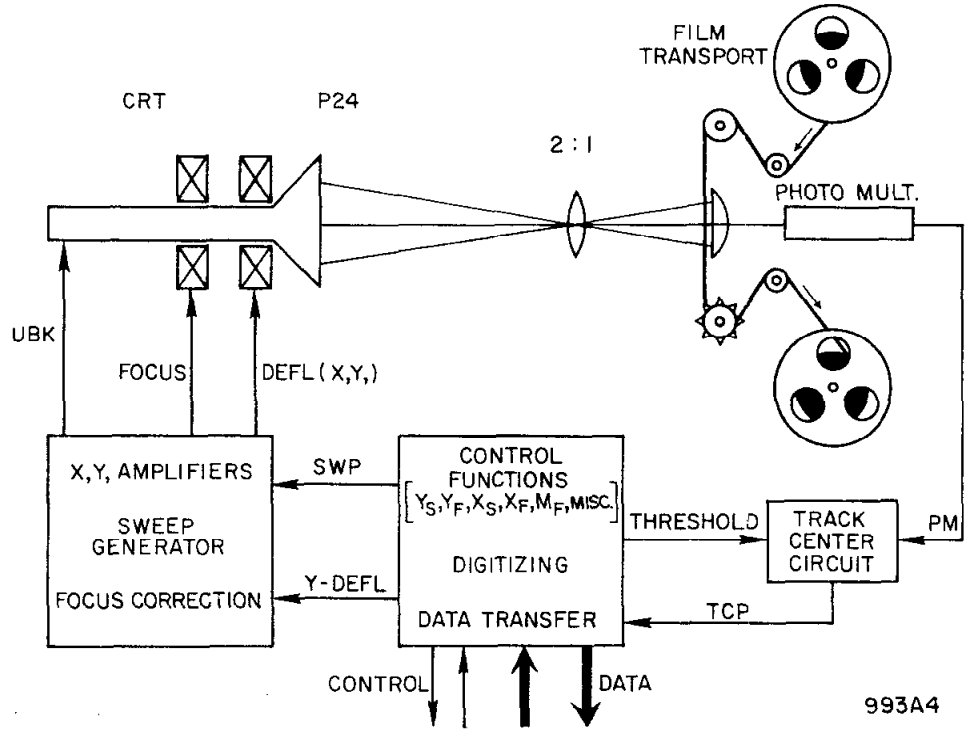

FIG. 3--Film reader block diagram.

in computer time to calibrate partially corrected hardware and scanning hardware with no correction at all is negligible. The film, therefore, is scanned in a distorted coordinate system in which local pattern-recognition of sparks and fiducial marks takes place.

The CRT coordinates are calibrated against a pattern of 54 crosses, shown in Fig. 4, the centers of which have been accurately measured on a manual measuring machine.

Corrections are performed on the spark and fiducial centers after these have been located and before linkage into tracks is made. The required accuracy is obtained by fitting a third-order polynomial.[2]

This calibration is to eliminate the inherent non-linearities of flat-faced cathode ray tubes, and optics distortions, and is done routinely at the beginning and end of a roll of film. Another correction is to be made for instabilities introduced by the CRT deflection system such as short-term drift and the positioning of the film. This correction is made on every frame by the measurement of three fiducials whose coordinates are independently known.

Another by-product of the flat-faced CRT is deflection defocusing. It is caused by a variation in length of the electron beam with deflection, and its effect has to be corrected for in the hardware. A correction current must be applied to the focusing coil in order to maintain (electrical) focus over the entire screen.*

The deflection coils of magnetically deflected CRT's exhibit a small amount of hysteresis (0.05%). This effect is particularly annoying if the spot were deflected randomly. In this case, however, where a TV-type raster is swept, the spot approaches the film data always from the same direction. In addition to this, an accessed rectangle on the film is always approached via the origin. The hysteresis effect does therefore not come into our corrections.

A P16 phosphor is commonly used in CRT flying-spot scanner applications because of its short persistence (0.1 μsec). Unfortunately, P16 has some severe drawbacks such as relatively low resolution, low light output, a large part of which is in the ultraviolet region of the spectrum which requires specially designed optics. In addition, an aging effect and the susceptibility to burning make this phosphor far from ideal. The P24 phosphor that has been used in the described equipment does have none of the above mentioned disadvantages, is

*Covered in detail in Part II of this report.

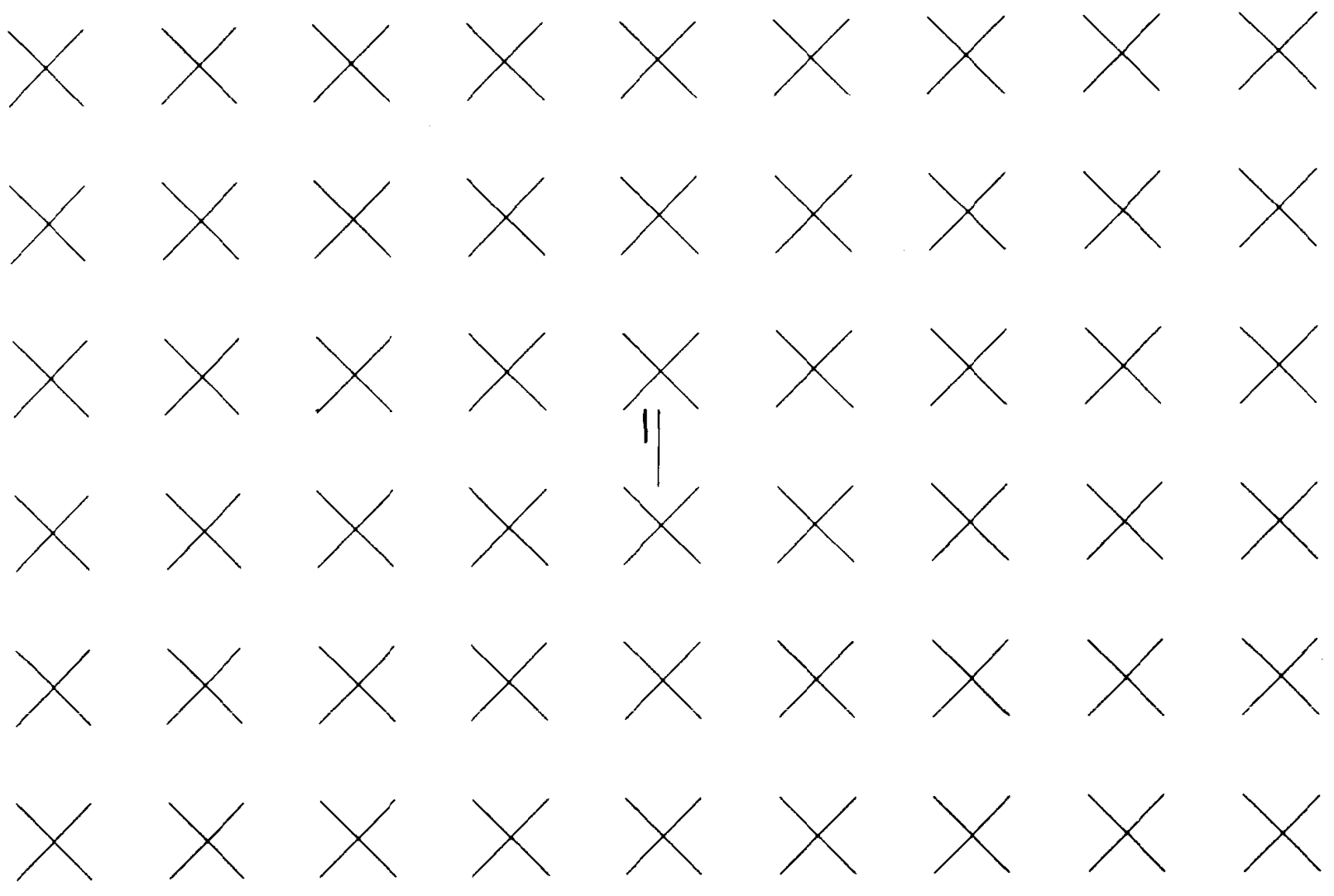

FIG. 4--Calibration pattern.

very efficient and emits light in the visible region, which simplified optical requirements and is very tolerant to maltreatment (burning); however, the persistence being 1 μsec to decay to the 10% point does not permit as fast a scanning speed as P16 would allow. With proper electrical filtering of the photomultiplier signal a sweeping speed of 36 μm/μsec may be used with reasonably good resolution.

Two filmscanners are operating, the first one of which uses a 5-inch CRT, the image of which is demagnified 2:1 onto the film. Only 35 mm perforated film is accommodated. The light passing through the film is collected by focusing the aperture of the objective lens on the cathode of a photomultiplier. Since a large ($\approx$ 10 mm diameter) spot is produced in this manner, local sensitivity variations of the photocathode, if they were present, would be cancelled out.

The second filmreader uses a 7-inch CRT and accommodates both 35 and 70 mm perforated film. The optics has unit magnification. Although the same basic principles underlie both Hummingbird I and II, some of the more significant differences are shown in Table 1.

TABLE 1

Comparison of Differences Between Hummingbird I and Hummingbird II

	Hummingbird I	Hummingbird II
Cathode ray tube with P 24	5-inch	7-inch
Least counts along one scanline	2^{12}	2^{14}
Scanline densities	1024/512	4096/2048/1024
Threshold on photomultiplier	16 levels	16 levels
Crystal controlled clock	2 Mc/sec	8 Mc/sec
Time per scanline	~ 2 msec	~ 2 msec
Scan speed on CRT	36 μ/μsec	36 μ/μsec
Scan speed on film	18 μ/μsec	36 μ/μsec
Optics	2:1	1:1
Digital resolution (no buffering)	36 μm	72 μm
Film transport (stepping motor)	~ .4 sec/frame	.4 sec/104 mm frame
Film size	35 mm	35 and 70 mm
Image size	36×24 mm^2	104×60 mm^2

In both machines the film is moved and positioned by a stepping motor. Two motors on the same axes as the reels are constantly under power, keeping the film taut. Idlers on swinging arms with a spring arrangement provide some buffering. Due to the low speed of film-movement no vacuum loops or servoing of the idler arms is required. The film is moved in either direction under program control and automatically centered in the filmgate to 1% of the length of one full frame. A frame-by-frame movement takes 0.4 second and positioning of the film is repeatable to ± 0.1 mm (nonaccumulative). Although the film advancing process is slow, especially in Hummingbird II where vacuum holddown of the film is applied, this arrangement is satisfactory since spark-chamber film is measured, that has not been prescanned so that each frame has to be examined. In addition the film advance takes place in parallel with the processing of the data of the previously scanned frame. A faster film transport, having vacuum columns for film buffering is now under construction and will be mandatory if prescanned bubble chamber film is to be processed. Figure 5 shows both machines. Figure 6 depicts the slow 70-mm film transport, while Fig. 7 shows the fast film transport under construction.

A. Data Transfer

The actual connection between the 360/75 selector channel and the scanning hardware takes place through an IBM 2701 which has been designed to enable the attachment of non-standard or non-IBM devices.[3] Data is transmitted through the execution of write instructions, while data is moved into the core by the execution of a read instruction. In this particular case the 2701 is transmitting and receiving data over a set of sixteen output and sixteen input lines respectively. Since the operation is asynchronous, a set of control lines serves to control the operation. If the 2701 is selected for a write operation a WRITE SELECT line is brought up, while the presence of a true level on the WRITE READY line indicates that there is valid data on the output data bus. The external device responds with a DATA DEMAND signifying the acceptance of the data. The WRITE READY line is dropped and again brought up if new data is being presented on the output bus. This process will continue until all data has been sent, which is indicated by a line WORD COUNT (WC) = 0 being true. At this time the external device responds with an end-of-record signal, thus freeing the channel.

The transmission of data into the 360 occurs in a similar manner. The 2701 is selected for a read operation bringing up the READ SELECT line, while the

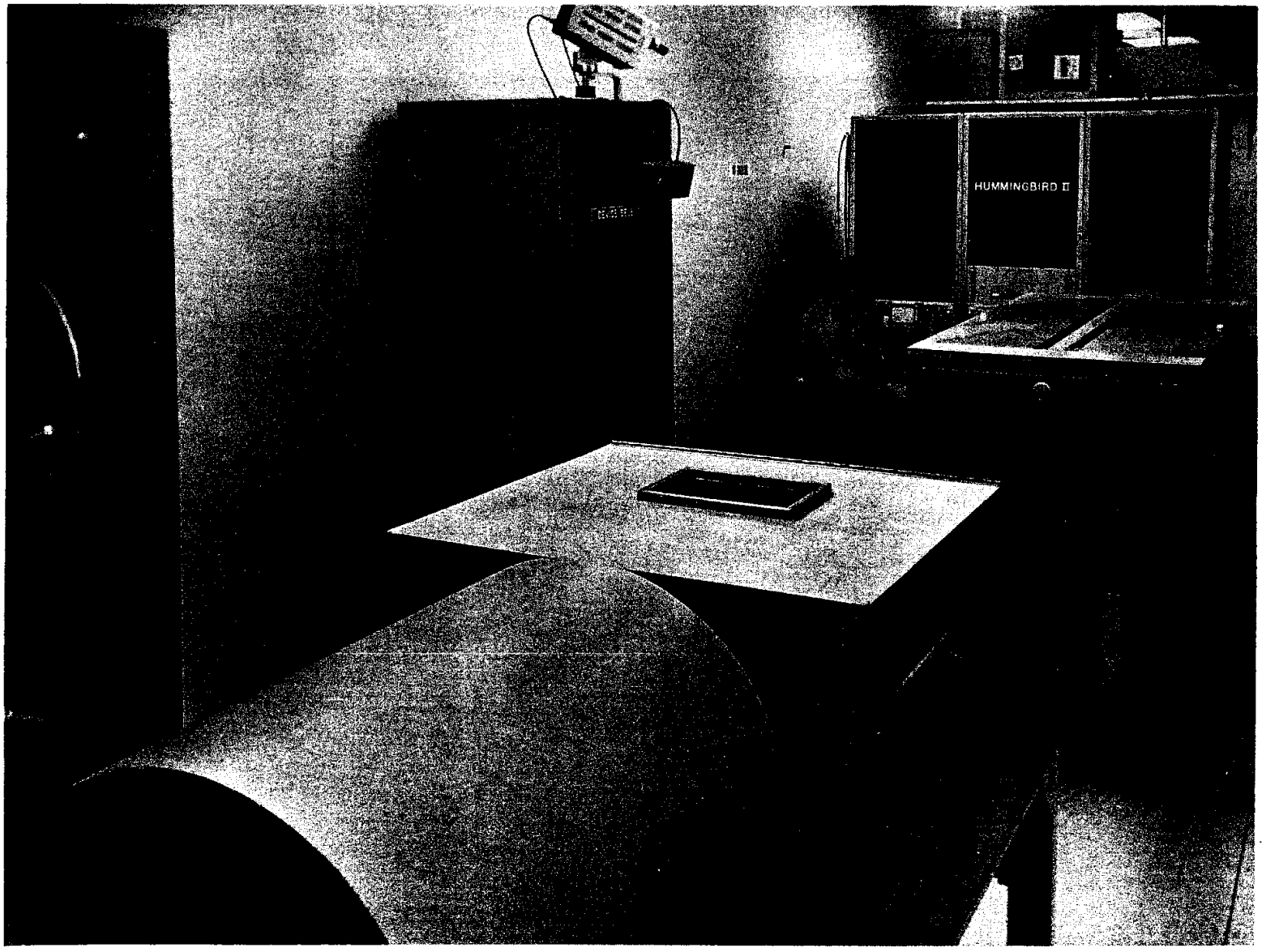

993A6

FIG. 5--Overall view of the graphic data processing laboratory.

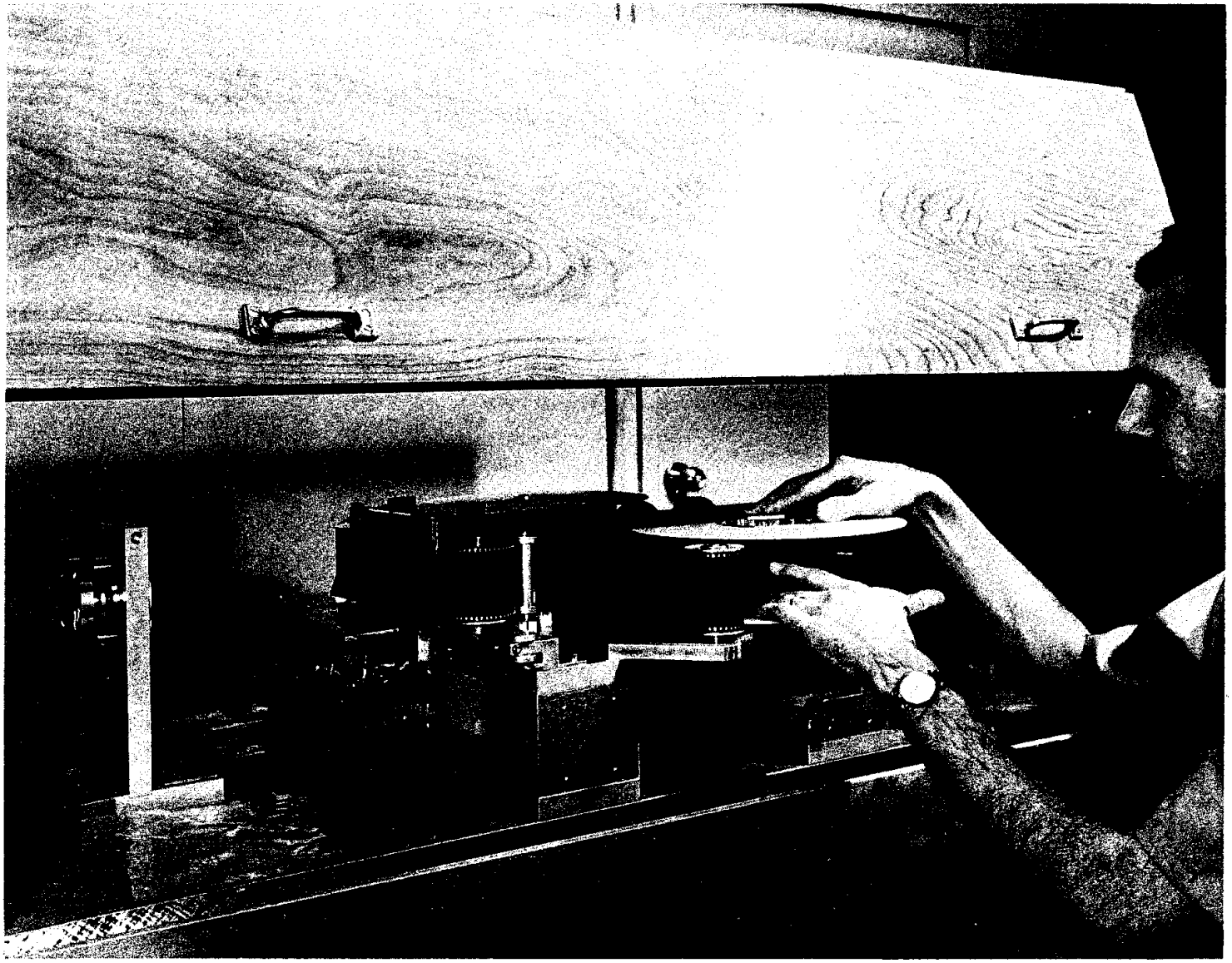

993A7

FIG. 6--Stepping motor driven film transport.

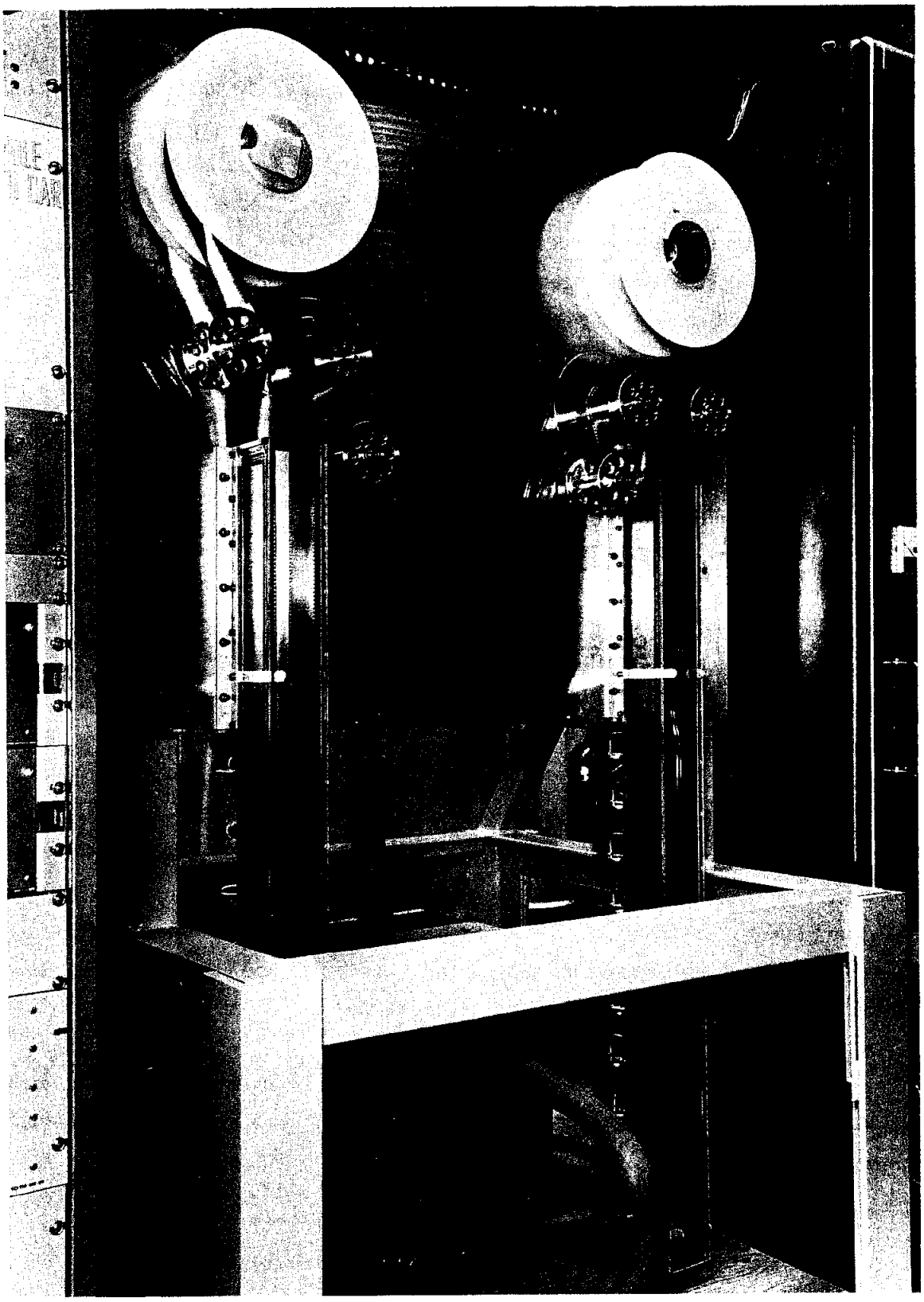

993A8

FIG. 7--Fast film transport under construction.

READ READY line signifies its readiness to accept data. In this case the DATA DEMAND line indicates to the channel that data is present on the input lines. Since it is unknown at the outset how much data is going to be sent, the WC = 0 line may not be used to signify the end of the data transmission, but rather the device itself terminates by sending an END OF RECORD at the end of its operation and the channel is disconnected. An INTERRUPT line is brought up by the external device when it requires attention. This would in this case occur at the end of a MOVE FILM operation during which time the channel is not connected and the computer is going about its own business. An END OF FILE line is available and is wired to a switch that senses the end of the film. This signal may also be given manually by the operator in case of an abnormal job ending, again to free the channel.

The IBM 360 channels transmit data in byte-form, that is eight-bit units. Two of these are assembled in the 2701 into one sixteen-bit half word. The speed of transmission is determined by the channel and is one byte per microsecond or 2 microseconds per halfword, which in fact turns out to be 2.2 microseconds.

A 2701 may have as many as four sixteen-bit ports, each with its own address. Although this system consists of more than one external device, only one port is used for economical reasons and because only one piece of equipment has to operate at one given time. A simple electronic switch has been built to allow for the attachment of eight devices to one 2701 with parallel data adapter. This "device selector" locks in on the very first word received on the output lines, determines the device number and routes all data to the selected device, disconnecting all others. A more detailed description may be found in Ref. 4.

B. Scanner Control and Digitization

Before the start of a film scanning operation the scanner is first to be selected and subsequently initialized. The orders that are sent in a sixteen-bit halfword are in the following format.

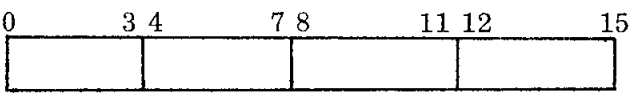

The first half byte, bits 0 through 3, contain the order that is decoded in the device, while the data is packed in bits 4 through 15. Eight orders have been

implemented, including one that is recognized by the device-selector.

Select (0) If all zeros are present in bits 0 through 3 on the very first word transmitted then this is interpreted by the device selector as a selection order. The actual device number is contained in bits 12 through 15. The device stays selected until another is selected. At present provision is made for only seven devices although there is of course no limitation.

As has been previously mentioned, the film is accessed in rectangles, a method which we have found to be particularly convenient and well-suited to the digitization of spark chamber film. The databox containing the picture number and possibly other useful information and arrays of different chambers may be accessed in turn. This selection could of course also be made in core after the whole frame has been digitized. An appreciable reduction in (not useful) data transmitted, however, is realized in this way, by preventing the digitization of hand written or picture number information for human interpretation.

The coordinate system of the filmreaders is shown in Fig. 8.

The four corners of each rectangle are specified by the orders YS(1), YF(2), XS(3) and XF(4) where the numbers between brackets denote the contents of bits 0 through 3.

YS(1) Loads the first line to be scanned by presetting the Y-counter with the contents of bits 4 through 15

YF(2) The last line to be scanned, in bits 4 through 15, is moved into the YF-register. A comparator detects identity upon which an end-of-record signal sent to the computer signifies the end of an area or subarea scan.

XS(3) No X-coordinates smaller than the value in bits 4 through 15 are transmitted.

XF(4) No X-coordinates larger than the value in bits 4 through 15 are transmitted.

The film positioning is entirely under program control. The film is moved in increments of 1/100 of the length of one full frame in either direction. The number of increments is loaded into a counter which is made to count down. If its content is zero the film is assumed to be in position and an ATTENTION INTERRUPT is generated after a short delay to allow for the vacuum hold-down

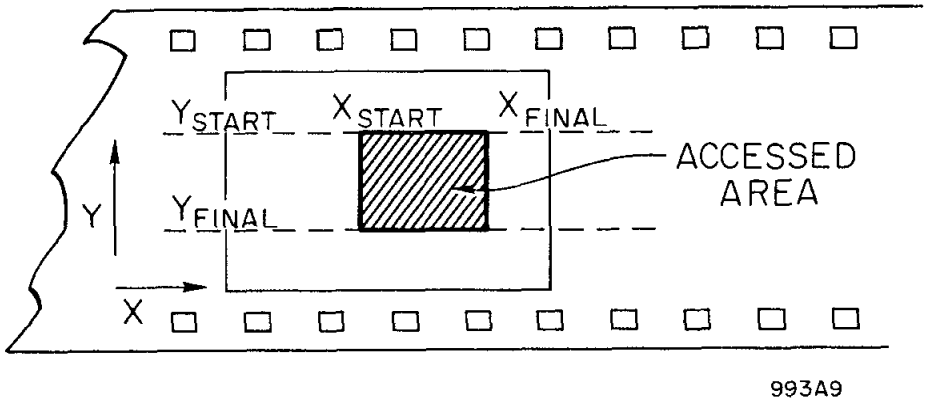

FIG. 8--Film reader coordinate system.

to occur.

MF(5) Moves the film the number of increments specified in bits 5 through 15, while bit 4 denotes the direction of movement.

After a rectangle has been specified, the density of scanlines, a threshold level to reject some background noise, and the scanline orientation, either along the edge of the film or perpendicular to it, still have to be specified.

MISC(6) The contents of bits 4 through 7 in this order identify one of sixteen threshold levels. Bits 10 and 11 specify the number of scanlines as either 4096, 2048, or 1024 over the whole frame, although a frame may of course only be partially scanned with a chosen density. A one in position 15 denotes the orthogonal scan direction.

CLR(7) All registers internal to the scanner are reset. This order is normally given after every select (0) order.

A COMPUTER WRITE operation, to transmit these orders, is terminated if no more bytes are to be sent as is indicated by the WC = 0 line, set by the program. The device responds with an END OF RECORD signal upon which the program starts the execution of read instructions. The scanner thus initialized will recognize the change from a WRITE to a READ operation, which it interprets as the signal to commence the scan. Completion of the reading of a frame or subarea as determined by the device is indicated with an END OF RECORD signal to the channel which in turn generates a CHANNEL END, DEVICE END. The transmission of data during a read or scanning operation occurs in a sequence which enables the program to determine the X- and Y-coordinates of the hits. Before the start of a scanline, its coordinate is transmitted, followed by the X-coordinates of the hits on the scanline. Scanlines are separated by the transmission of a word containing all zeros.

The data transmission is in the following format with Y being the scanlines and X the hits on a scanline:

$$0,\ Y_n,\ X_1,\ X_2\ \text{----}\ X_m,\ 0,\ Y_{n+1},\ X_1,\ \text{etc.}$$

A linear sweep moves the spot along a scanline. Concurrently with the sweep, a crystal controlled clock feeds into the X-counter. The contents of the X-counter represent the position of the spot along a scanline at any given time. The spot swept over the film produces a signal at the output of a photomultiplier. After proper electrical filtering the center or midpoint of a pulse is determined by

means of circuitry. This track center point is, after synchronization with the clock, used to strobe the contents of the X-counter into the output register, if the X-value lies between XS and XF, for subsequent transmission. Since the coordinates are transmitted directly from the output register, no new X-coordinate is read until the previous one has been accepted by the channel. This limits the (digital) resolution and is a function of the spot speed and maximum channel rate. A small amount of buffering would eliminate this problem although this has not been implemented at this time. At the end of a scanline the Y-counter is advanced. Its contents are converted into an analog voltage for deflection in the Y-direction.

C. Performance of the Film Reading Equipment

The precision measuring ability of CRT flying-spot devices, connected on-line to computers, is not as much a matter of linearity as of repeatability, i.e., stability of the device. The inherent nonlinearities of the CRT, the optics and its alignment may, by relatively simple calibration procedures and calculations, be corrected to within the desired tolerances. The time interval between calibrations is, however, a function of the stability of the hardware. By keeping the analog circuitry of these devices to an absolute minimum, but of high quality, a great deal of stability is obtained.

The lateral and longitudinal stability, although important, is not critical since a correction is introduced on each frame for film positioning errors to which it is equivalent. Size changes or gain variations are of greater consequence, because they determine the frequency of calibration. A simple test has been designed to illustrate the gain stability using the calibration pattern of Fig. 4. The variations in the X and Y positions of the calculated centers of two diagonally opposed crosses have been plotted against time. (See Fig. 9(a) for the Hummingbird I and Fig. 9(b) for the Hummingbird II.) Although the environment is air conditioned, no special precautions have been taken to insure an absolutely constant temperature and humidity level.

Another critical requirement for these film readers is resolution. Although many methods of measuring resolution or spot size exist, none is generally accepted. In addition, the tagging of a spot with a number is quite meaningless, since it greatly depends on where, on the CRT face this measurement took place, while also personal judgement is sometimes involved. Neither does it take into account the spot degradation by the optics. Since the most critical test for these machines from a resolution point of view is the scanning of bubble chamber film,

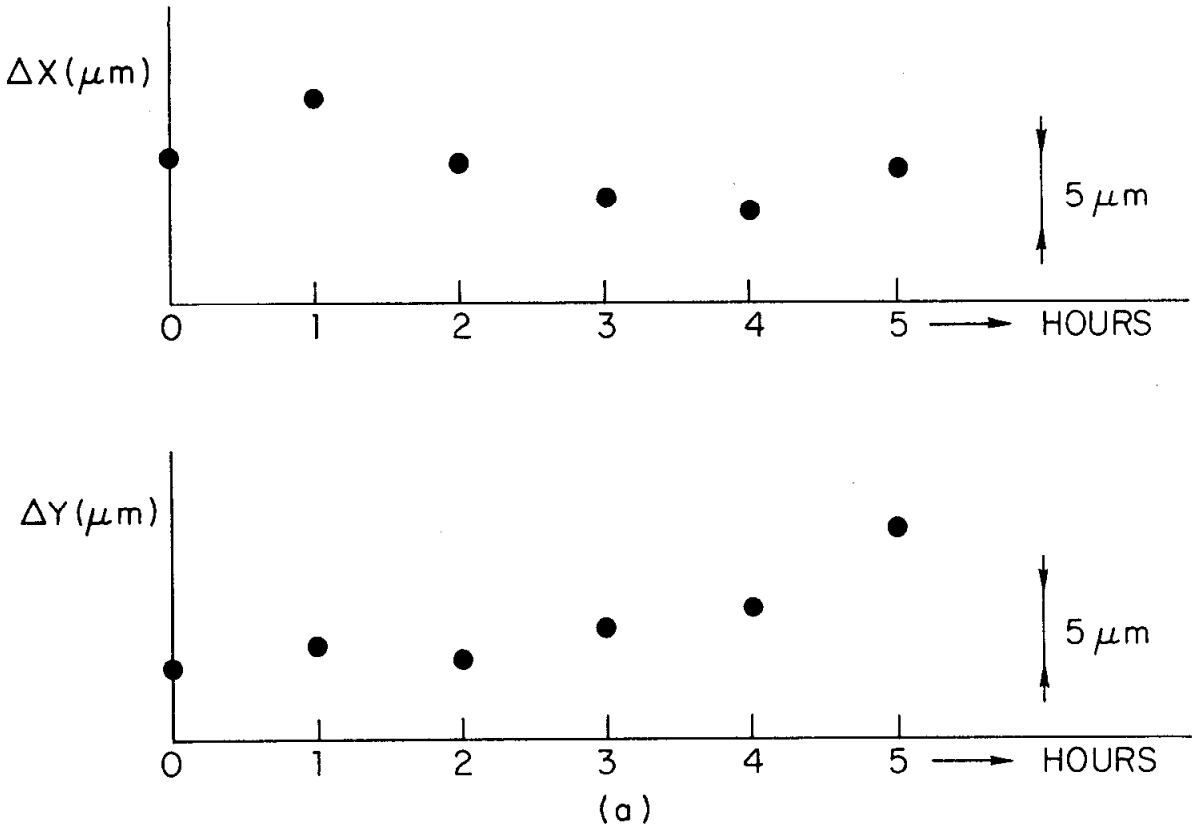

FIG. 9a--Hummingbird I stability plot.

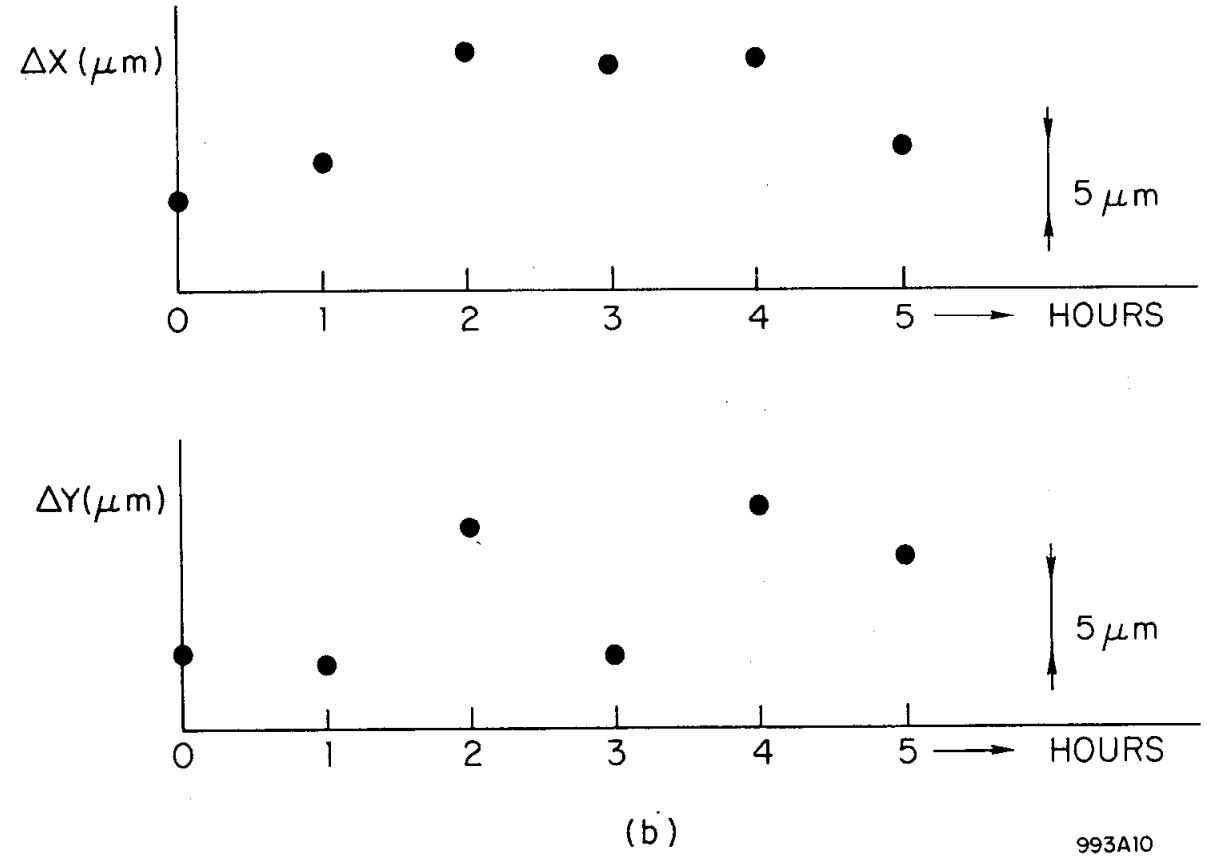

FIG. 9b--Hummingbird II stability plot.

we have chosen to illustrate the total systems resolution by comparing the original frame with its playback. The right bottom photograph of Fig. 1(b) shows a view of the Brookhaven 20-inch chamber at about actual size. An off-center subarea, measuring 5×10 mm^2, off the films, is shown with its playback in Figs. 10(a) and 10(b), while Fig. 11 gives an idea of the photomultiplier signal before and after conditioning, when the spot is swept over the film. The bubbles are typically between 20 and 30 μm in size.

D. Hummingbird IX

The mode of operation of these film reading devices is tuned to the accurate digitization of spark and bubble chamber film. On these films the presence or absence of data and its location with respect to some known references marks are of importance.

For various other applications, disparate information such as a digitized grey scale is needed. In these cases the precise digitization of the location is generally of lesser significance. In particular some work has been done on the experimental analysis of film for medical purposes such as X-ray film and chromosome pairing. A point sampling mode of operation seems to be more advantageous for these applications. Although the Hummingbird device is not well suited for operation in this mode, it can be easily simulated by taking light samples along a scanline at approximately equal distances. At present, 1024 such samples may be taken along a scanline in two successive scans, while a total of 1024 lines may be scanned. This produces a 1024×1024 point raster, of which a subdivision into smaller rectangles might be performed in exactly the same manner as in the "normal" mode of operation.

The grey scale is digitized in eight equally spaced sublevels that lie in a band, the width of which is specified in the program by setting a minimum and a maximum level. Figure 12 shows the original and a printer plot generated from data obtained in this manner.

E. Display Equipment

Computer-driven displays are found to be increasingly useful in graphic data analysis systems such as the one described. A great deal of use has been made of the IBM 2250 display unit, which forms part of the configuration of the 360/75. In fact, the operation of the scanning equipment is controlled entirely from the console of the 2250. Great flexibility in setting the scanning parameters as well as immediate playback of the data taken off the film have proven invaluable in the

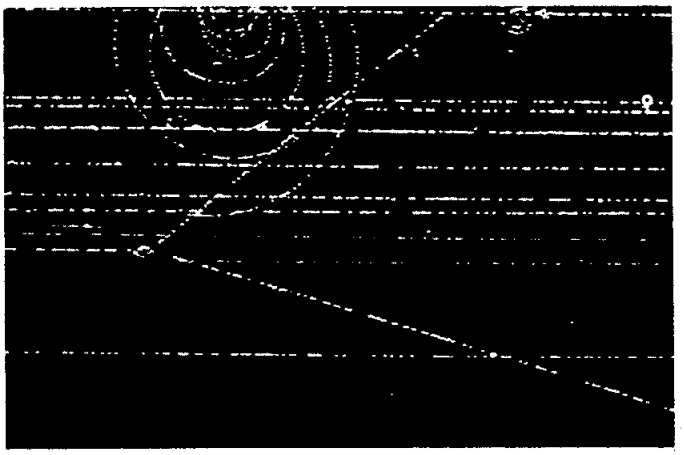

FIG. 10a--5 × 10 mm^2 bubble chamber film.

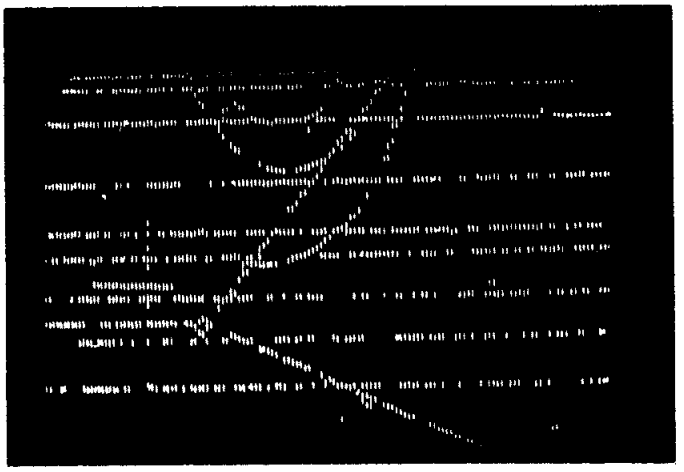

993A12

FIG. 10b--5 × 10 mm^2 bubble chamber film and playback.

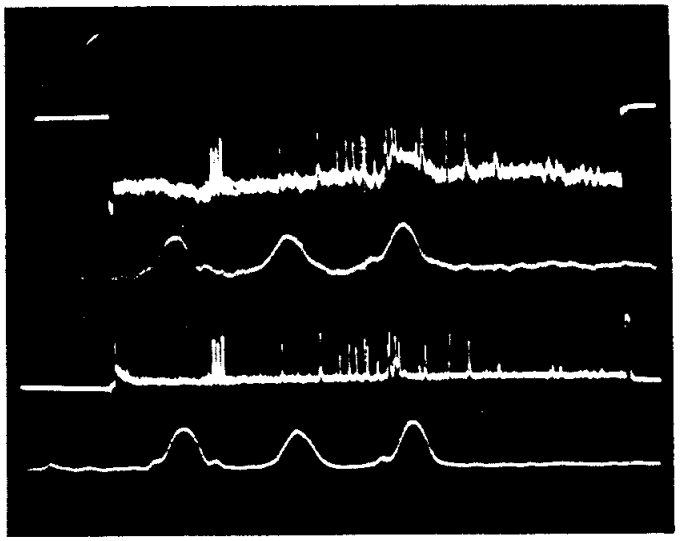

993A13

FIG. 11--Raw and filtered PM signals of bubble chamber film.

FIG. 12--Original film and a hummingbird generated printer plot (incorrect scaling).

engineering stages as well as for program diagnostics. Unfortunately the use of the 2250 requires a great deal of interaction with the large computer and the operation of the latter. This is tenable if such interaction is sporadic and just for debugging purposes, but becomes inconvenient when the film analysis system will be used in production.

Even in the most successful film data processing system one has to contend with a number of rejects, photographs that for one reason or another have the programs confused, causing them to produce incorrect answers. These rejects are stored on a magnetic tape during a production run and are subsequently studied, and possibly corrected off-line on a special purpose display with light-pen. This display, referred to as the twenty-two and a half, (see Fig. 13 and 14) is a point plotting display and has an internal refresh memory of 4096 words of 32 bits each and a cycle time of 8 μsec. The display is continually cycling through its own core, enabling the operator to perform the necessary lightpen tagging off-line, thus minimizing the interaction with the large facility. Upon completion of his task the operator pushes the INTERRUPT button, generating an ATTENTION INTERRUPT in the 360/75, upon which the program will unload the event presently in the display core and load a new event for subsequent analysis. The corrected events are then to be merged with the previously measured ones. A similar system is in operation at Brookhaven National Laboratory using a drum as the refresh memory for the display unit. The 21-inch rectangular cathode ray tube is magnetically deflected and electrostatically focused. The 32-bit word of the internal core storage is divided into a left and a right halfword, for the X- and Y-coordinates respectively. The twelve right most bits of each halfword are converted into analog voltages for the deflection and the four bits preceding these are used for special functions. The format:

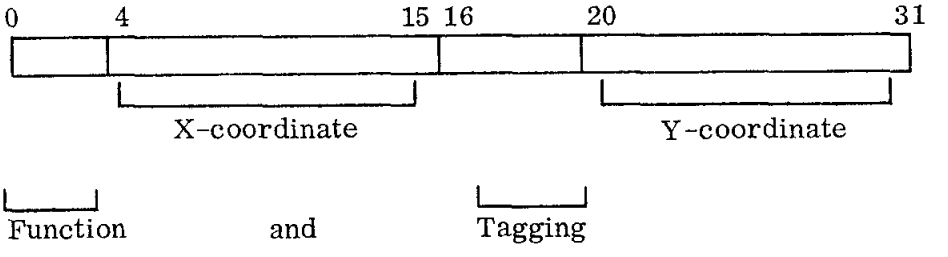

A one in position 0 prevents the data from being displayed. A one in position 16 means that that particular data word has been tagged by the lightpen and should

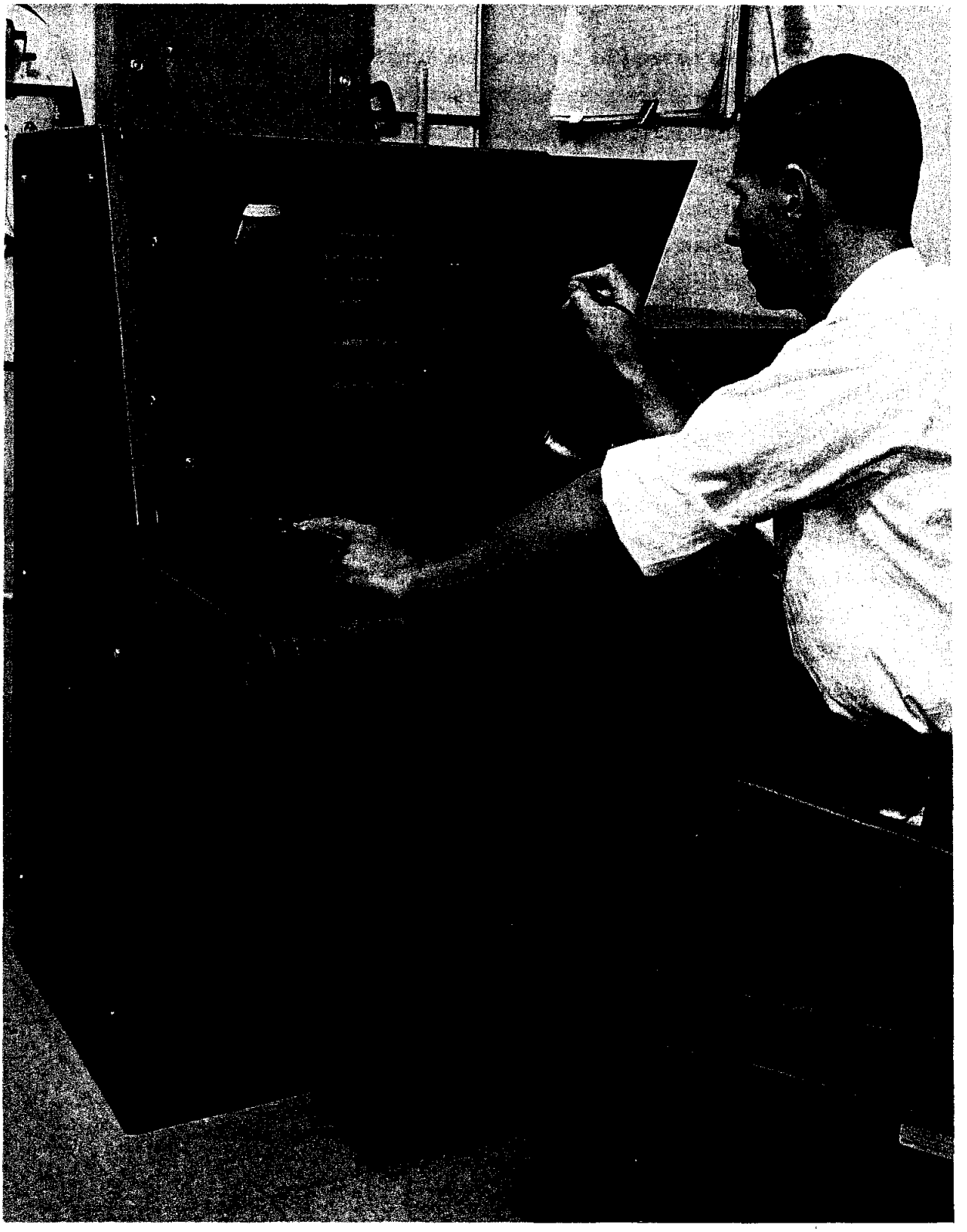

993A15

FIG. 13--Interactive point plotting display console.

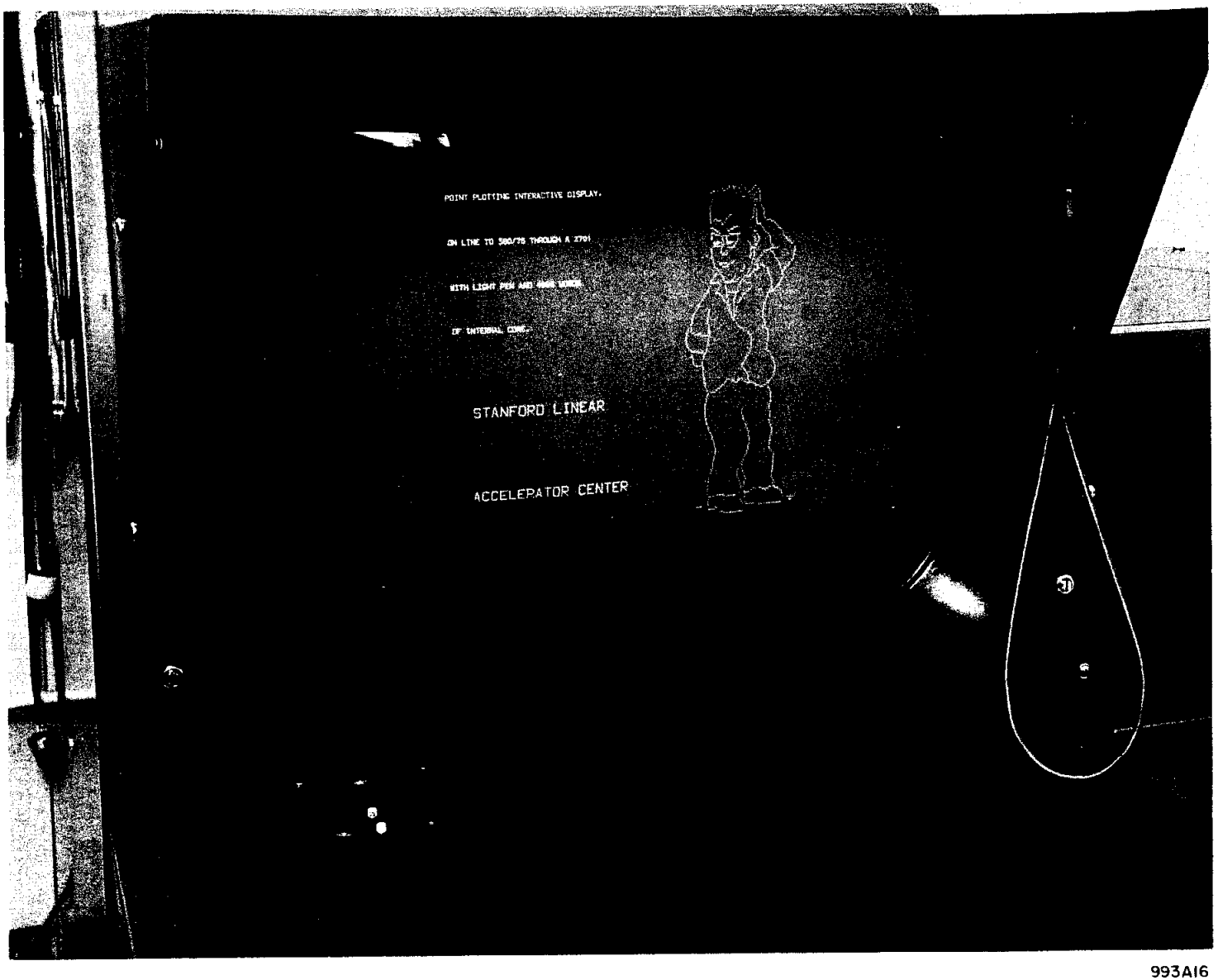

993A16

FIG. 14--Closeup of Fig. 13, showing function keys and light pen.

be brightened. A one in position 17 disables the lightpen for that word. If a one is present in position 18, it will cause the data that has been tagged by the program or the lightpen in position 16 to blink at a rate of three times per second to draw the attention of the operator. The remaining bits will be used for character generation and vector drawing that have not yet been implemented.

The 32-bit word, read out of the internal core, is strobed into register one (R1) and jam transferred into register two (R2). Two registers are used to generate some overlap in the time needed for memory read out and the time necessary to deflect the electron beam. The memory is read into R1 while the data is displayed from R2 as well as reloaded into the memory. Although the time the amplifiers need for maximum deflection is 30 μsec, a scheme has been devised to shorten this time for coordinates that are closer together than the maximum distance. This has been made possible, because of the availability of the two registers mentioned above, since R1 at a specific point in time contains the "future" coordinates of the beam while R2 holds the present location of the spot. The time for deflection has been made almost linear with the distance travelled. By examining the two most significant bits of X and Y in both R1 and R2, the total CRT screen is divided into sixteen virtual rectangles. The time necessary to move the electron beam is derived from the data to be 8 μsec to move within one box, 16 μsecs to go to an adjacent box, 24 μsecs to jump one box and 32 μsecs to jump two. The net result of this "collate" system is that the average time per point displayed is significantly reduced.

The computer display program may, by arranging the data for a minimum number of border crossings, assist in this optimization process.

The lightpen on this particular display has been designed to flag data, rather than to generate an interrupt upon detecting light on the CRT face. The data that is seen by the lightpen is immediately brightened, providing guidance to the operator. Conversely data that has been marked may be erased to eliminate overshoots in the filtering process. The brush action of this lightpen is extremely valuable to facilitate the manual filtering process in which the tracks of interest are to be separated from crossing tracks or other data, interfering with the automatic filtering program.

The display is connected to the device selector, which in turn is connected to the IBM 2701 for the transfer of data from the 360/75. After the device has

been selected with the very first word of a block of data, the integral display memory is loaded with data in sequential addresses, always starting at location zero. A transmission is terminated with the WC = 0 signal from the 2701 upon which an END OF RECORD is generated. Since loading and unloading of the memory always starts at location 0, this enables a partial update of the data starting with location 0.

II. PRECISION CATHODE RAY TUBE DEFLECTION SYSTEMS

Precision cathode ray tube deflection systems are generally of the magnetic type. Although an electrostatic deflection system would be less expensive and not as bulky as a magnetic deflection system, this choice is dictated by the imaging process which generates the spot on the screen.

Assuming an optimum cathode current density, a smaller and more intense spot can be obtained by increasing the angle of convergence θ of the beam at the screen. However, for a given θ, deflection defocusing appears to be more serious for electrostatic deflection than magnetic deflection, due to the fact that in the latter case deflection is performed with a more uniform field; indeed the size of the field producing element is not limited. Furthermore, as they are acted on, the electrons keep a constant energy when magnetically deflected and this also contributes to a better focusing.

A. Tube Geometry and Deflection Distortions (Fig. 15)

The radius R of the beam curvature is found from:

$$\frac{m\nu^2}{R} = \nu e B \tag{1}$$

with

- ν electron axial velocity
- B magnetic induction, assumed uniform over the length L of the deflection coil
- e charge of the electron
- m mass of the electron

ν is eliminated in (1) by the use of the conservation of energy relation:

$$\frac{1}{2} m\nu^2 = eV \tag{2}$$

- V acceleration potential

The expression for R becomes:

$$R = \frac{1}{B} \sqrt{\frac{2mV}{e}} \tag{3}$$

The deflection angle γ is given by:

$$\sin \gamma = \frac{L}{R} = BL \sqrt{\frac{e}{2mV}} \tag{4}$$

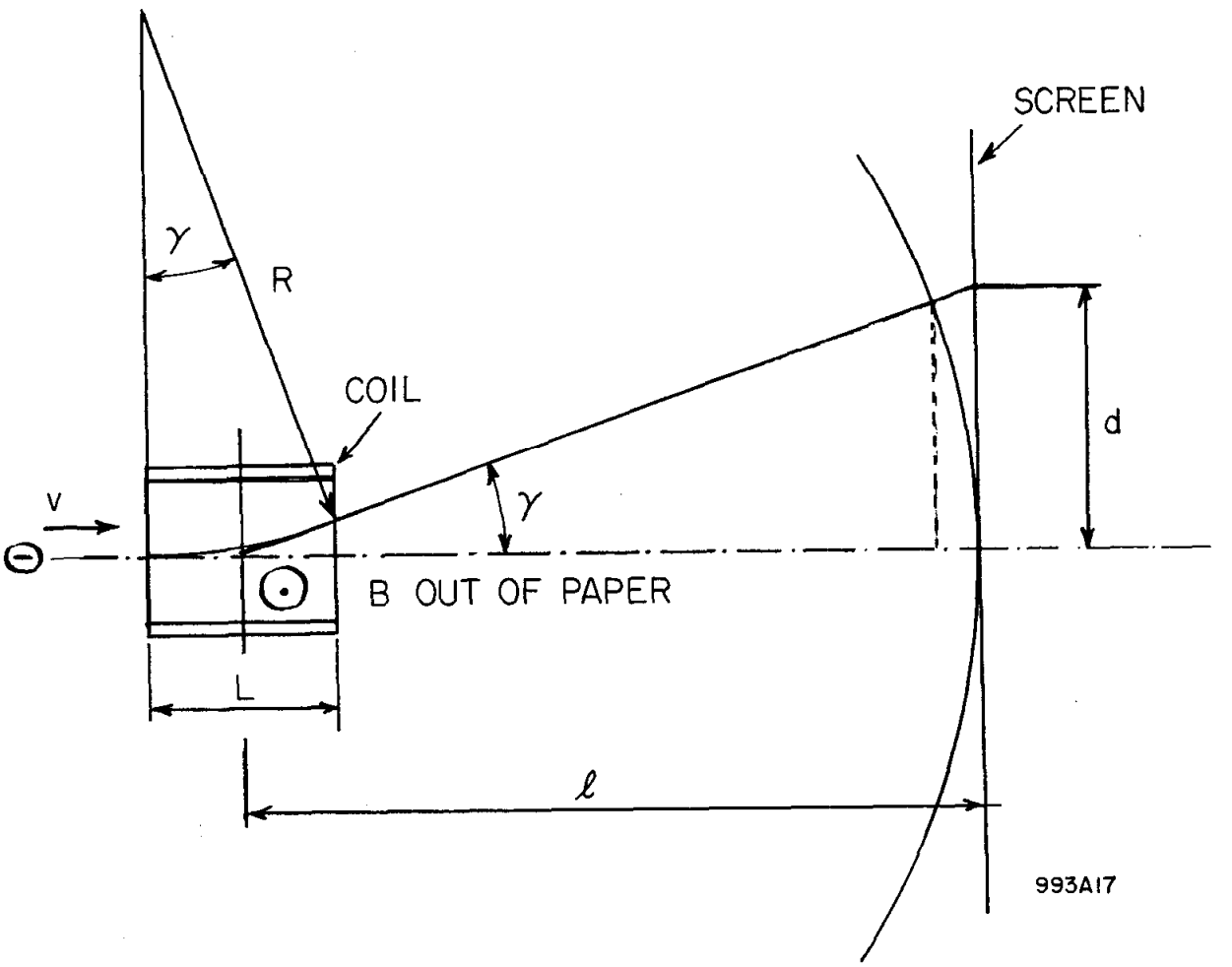

FIG. 15--Deflection system geometry.

For optical reasons the screen is made nearly flat. With d being the deflection on the screen, and ℓ the distance from the coil center to the screen, we have:

$$\tan \gamma = \frac{d}{\ell} \tag{5}$$

The so-called "pin-cushion" effect is entirely described by relations (4) and (5): the sinus of the deflection angle is proportional to the field or to the coil current, whereas the screen deflection is proportional to the tangent of the deflection angle. For small angles, sinus and tangent functions track each other fairly well, but for $\gamma = \pm 21^{\circ}$, a commonly used deflection angle, the error on d is:

$$\frac{\Delta d}{d} \times 100 = \frac{\tan \gamma - \sin \gamma}{\frac{1}{2}(\tan \gamma + \sin \gamma)} \times 100 = 7\%$$

Should the coil currents be made non-linear by multiplying them by some function $F(\sin \gamma)$, it would be possible to obtain a linear deflection system. Indeed we have:

$$d = \ell \tan \gamma = \ell \frac{\sin \gamma}{\sqrt{1 - \sin^2 \gamma}}$$

$$d = \ell \sin \gamma \left[1 + \frac{1}{2} \sin^2 \gamma + \frac{3}{8} \sin^4 \gamma + \frac{15}{48} \sin^6 \gamma + \ldots\right] \tag{6}$$

The bracket represents the desired function $F(\sin \gamma)$. Evaluating again the error on d for the case $\gamma = \pm 21^{\circ}$, the complexity of the "linearization" becomes obvious:

$$\frac{\Delta d}{d} \times 100 = \frac{\sin \gamma \times 100}{\frac{1}{2}(\tan \gamma + \sin \gamma)} \left[\frac{1}{2} \sin^2 \gamma + \frac{3}{8} \sin^4 \gamma + \frac{15}{48} \sin^6 \gamma + \ldots\right]$$

$$\frac{\Delta d}{d} \times 100 = 6.18\% + 0.58\% + 0.06\% + \ldots$$

For an accuracy of 1 part in 4000 (0.025%), the function $F(\sin \gamma)$ should include one more term. The reduction of the "pin-cushion" by hardware manipulations is therefore very difficult. The only practical solution consists in calibrating the deflection system with a known pattern, and program the corrections accordingly, in the software.

Accelerating Voltage Stability. Deflection being proportional to $V^{-1/2}$, the requirement for the high voltage power supply stability is therefore $2(\Delta d/d) \times 100$ per cent. The Hummingbirds' power supplies have been selected with a stability of better than 0.01%.

B. Deflection Amplifiers

Current Source. The only way to control accurately the coils' current is to connect them to a current source. The higher the output impedance of the source, the higher the current stability and the faster the response. Figure 16 shows a current amplifier with an input impedance h_{11}, an output conductance h_{22}, and a current gain h_{21}. The outside connections are such as to feed back part of the output current to the input. Under these conditions the overall transconductance is found to be:

$$G = \frac{I_L}{V_s} = \frac{1}{R_0} \frac{R_F}{R_s} \frac{AB}{1 + AB} \tag{7}$$

I_L load current
V_s source voltage
R_o sampling resistor
R_F feedback resistor
R_s source resistor
AB complex loop gain

It is clear from Eq. (7) that the expression

$$\frac{AB}{1 + AB}$$

which is frequency dependent, represents the departure of G from the value:

$$\frac{R_F}{R_0 R_s}$$

For large values of AB, the coil current will essentially be:

$$V_s \frac{R_F}{R_0 R_s}$$

provided the three resistors R_s, R_F and R_0 are true linear resistors.

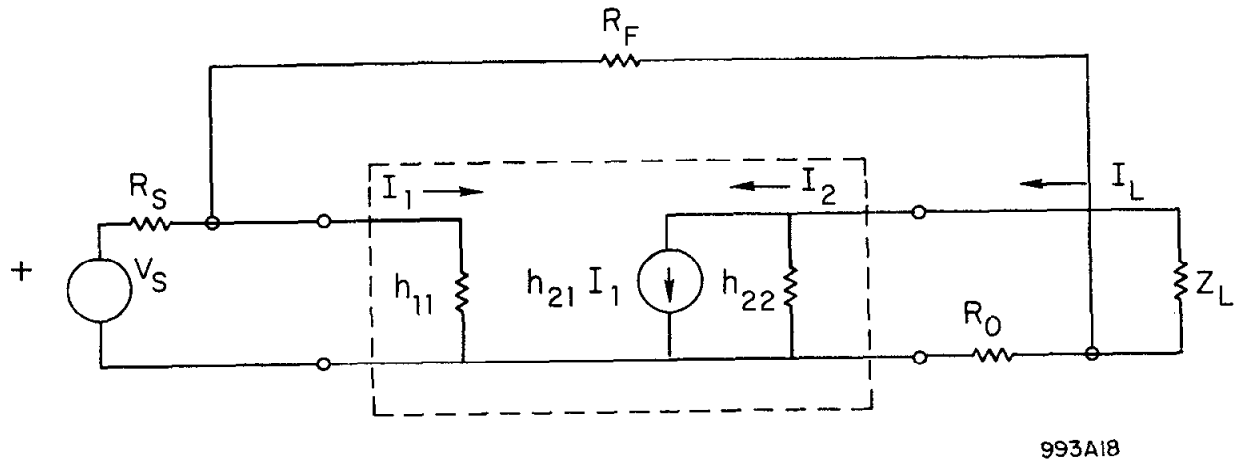

FIG. 16--Description of current source.

With no approximation except $\frac{R_0}{R_F} \ll 1$, one obtains:

$$G = \frac{I_L}{V_s} = \frac{1}{R_0} \frac{R_F}{R_s} \frac{AB}{1 + AB} \tag{7}$$

$$AB = h_{21} R_0 \frac{R_s}{R_s + R_F} \frac{\frac{1}{h_{22}}}{\left(R_0 + Z_L + \frac{1}{h_{22}}\right)\left(h_{11} + R_s // R_F\right)} \tag{8}$$

$$Z_{out} = R_0 + \frac{1}{h_{22}} \left[1 + h_{21} R_0 \frac{R_s}{R_s + R_F} \frac{1}{h_{11} + R_s // R_F}\right] \tag{9}$$

Note that in fact:

$$Z_{out} \cong R_0 + \frac{1}{h_{22}} (1 + AB) \tag{10}$$

when

$$Z_L + R_0 \ll \frac{1}{h_{22}} \quad .$$

One can also see that the source output impedance increases with the loop gain. The specification of AB is therefore necessary and will be determined from the deflection amplifier requirements.

Deflection Amplifier Requirements. We will examine first a typical dynamic requirement. For instance, the reference signals for horizontal and vertical amplifiers might be generated by a logic system using 12 bit shift registers. In this case the amplifier gain stability should be at least one part in 4000 at the frequency of interest. For a TV-type scan the required bandwidth would be of the order of 2 kc/sec, and for a point-by-point scan, a small signal rise-time of the order of 0.5 μsec would be desirable; this is equivalent to a bandwidth of 700 kc/sec.

This example would therefore impose the following requirements on the loop gain: its magnitude should be higher than 4000 (72 dB) at 2 kc, and become unity (0 dB) at 700 kc.

As concerns the static requirements, it was felt that long term drift should be as small as possible, perhaps of the order of 10 times better than the gain stability. In the case of the Hummingbirds, this will allow for less frequent calibrations of the deflection system.

Coil Selection. A deflection coil is characterized by the deflection angle it can achieve for a given current, by its inductance, resistance and distributed capacitance. When adding in parallel the capacitance of the connecting cable, the resonant circuit obtained constitutes Z_L. The resonant frequency f_0 should be higher than the maximum operation frequency, since for $f = f_0$, half of the source current is by-passed by the total load capacitance and does not produce any deflection.

Coil Data. Statistics for coil data are shown in Table 2.

TABLE 2

Coil Data

	H.B. I	H.B. II	Twenty-Two and a Half
L in μH at 1 kc	250	25	40
C in pF	180	60	70
R in ohms	1.0	0.15	0.18
I in Amps for 21° at 27 kV	2.0	6.2	7.6 (90° at 10 kV)
f_0 in Mc with 6-foot RG22 cables	0.6	2.5	2.0

Loop Stability. In view of the specifications outlined above, Eq. (8) gives the magnitude of h_{21}. Indeed with

$$|AB|_{\omega = 0} > 4000$$
$$R_0 = 2.4 \text{ ohms}$$
$$R_s = 1/2\ R_F = 2000 \text{ ohms}$$
$$h_{11} = 1000 \text{ ohms}$$

we obtain $h_{21} \geq 10^7$

Such a current gain requires four stages of amplification. Therefore AB will be of the form:

$$AB = \frac{|AB|_{\omega = 0}}{\left(1 + j\frac{\omega}{\omega_1}\right)^2 \left(1 + j\frac{\omega}{\omega_2}\right)\left(1 + j\frac{\omega}{\omega_3}\right)} \qquad (11)$$

with ω_1 and ω_2 standing for the 3 dB bandwidth of the low level stages and ω_3 standing for the 3 dB bandwidth of the output stage.

When the expression for AB is introduced into the equation for Z_{out}, Eq. (10), it is clear that at some frequency between ω_1 and ω_2, we have: Real part of $Z_{out} < 0$; that is to say, the amplifier will oscillate, and the loop gain function must therefore be modified in amplitude and phase. This problem has been treated in detail in Ref. 8 and will not be reproduced here.

Circuit Description and Performance. The schematic of Fig. 17 illustrates a typical current source which is used for the two H. B.'s and the 22-1/2 CRT.

The input stage is a silicon matched pair which exhibits a differential drift of 10 $\mu V/^oC$. Since the amplifier is operated as a voltage-to-current converter with a voltage gain of 2, the first stage drift will appear at the output multiplied by 2, whereas the following stage drifts will be reduced by the gain of the stages preceding them. A dc loop gain of 75 dB can be obtained yielding a close loop response down 3 dB at 1 Mc/sec.

For peak output currents of 50 mA, the rise time is better than 0.5 μsec with a maximum overshoot of 10%; indeed the loop phase does not exceed 120^o after corrections as shown on the Nyquist plot of Fig. 18.

The amplifier drift was found to be of the order of $\pm$ 50 $\mu V/^oC$ over a period of eight hours. This figure could have been reduced by decreasing the input impedance and the stage quiescent current, but these two solutions are not

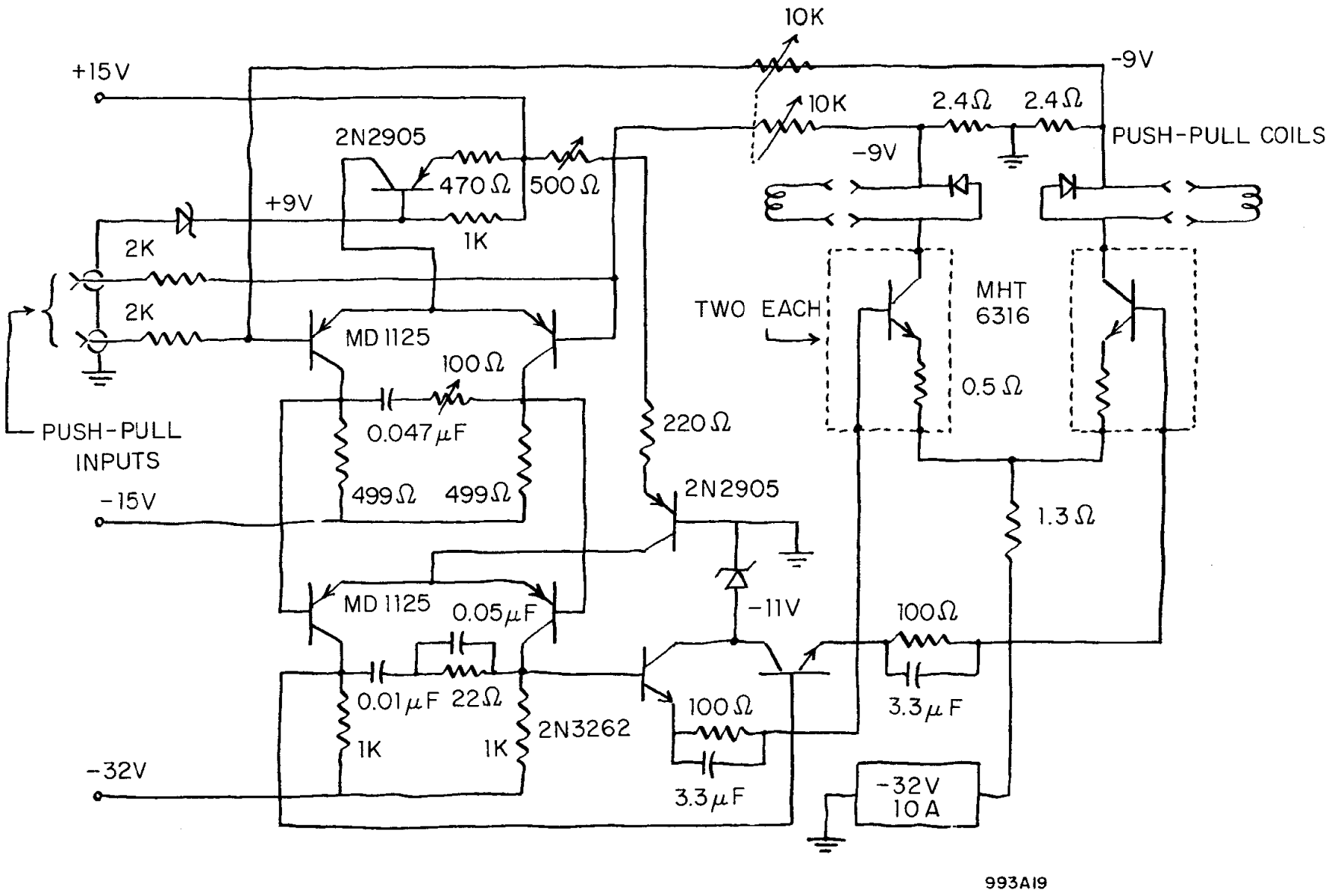

FIG. 17--Deflection amplifier.

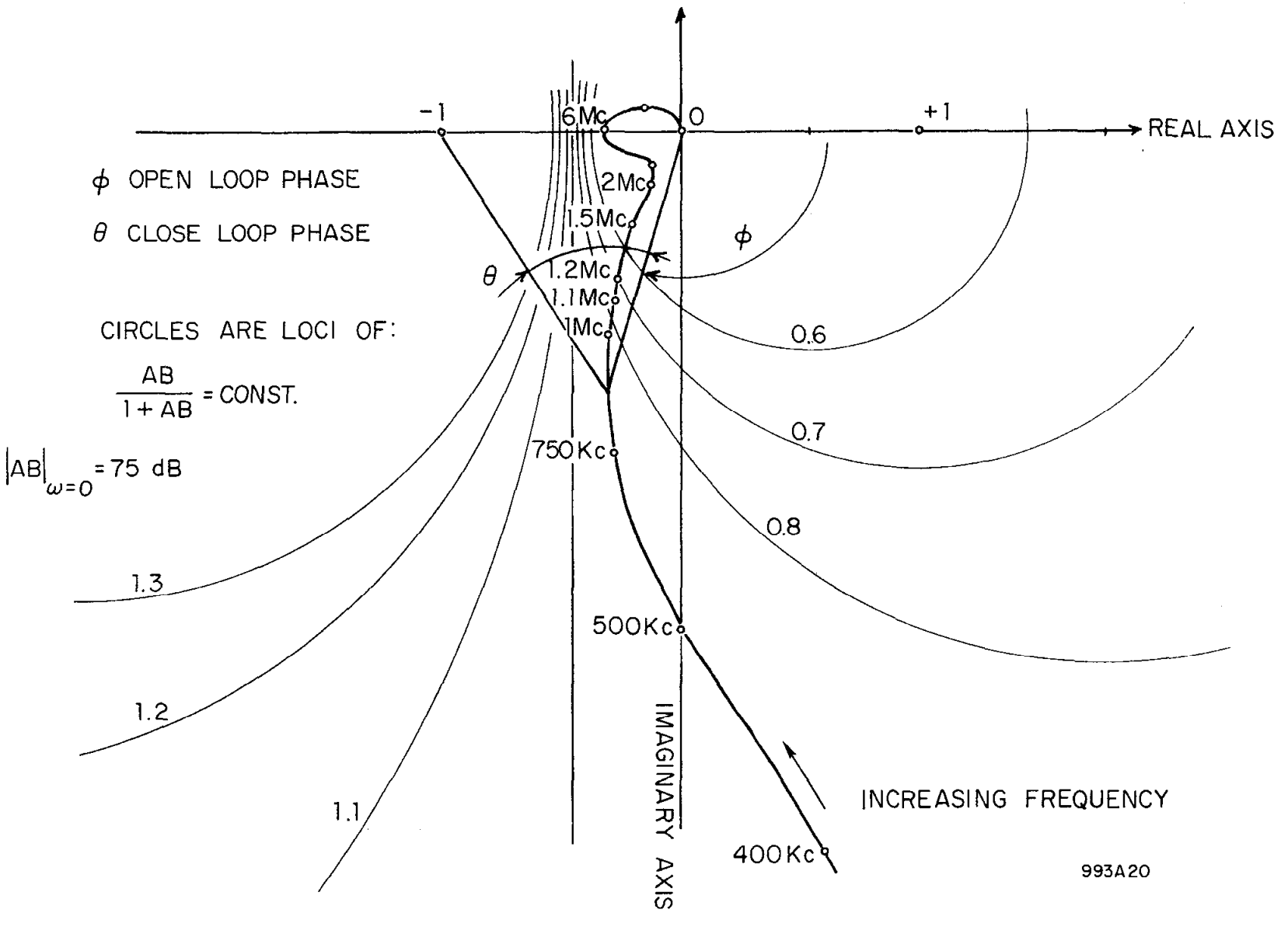

FIG. 18--Nyquist diagram.

compatible with an optimum gain-bandwidth product. The actual compromise is still satisfactory since it represents a drift of 1 part in 100,000 when the temperature varies between ± 2°C.

Amplifier Construction Detail. It is absolutely necessary that resistors R_0 (see Fig. 16) be perfectly linear and independent of temperature. If this were not the case the amplifier would no longer be of the constant current type, the feedback signal becoming of voltage type rather than current type.

Each resistor R_0 was made of 12 50-watt resistors in parallel, having a temperature coefficient of 5 PPM/°C; the two resistors are mounted in such a way that their temperature is essentially the same.

C. Focus Corrections

Dynamic Focusing. If ν_r is the radial component of the electrons velocity, the application of a longitudinal magnetic field will produce an helicoidal trajectory of radius r such that:

$$\omega = \frac{\nu_r}{r} = \frac{eB_z}{m}$$

ω angular velocity of electrons on helix

B_z applied focusing field (Fig. 19).

The period in the z direction is therefore:

$$T = \frac{2\pi}{\omega} = \frac{2\pi m}{eB_z} \qquad (12)$$

Focusing occurs if electrons hit the screen after traveling a distance ℓ in time interval nT. But as the beam is deflected, the distance increases to $\ell + \lambda$ and the period must be increased also to maintain focus. This is achieved by reducing B_z.

The defocusing effect can be expressed as:

$$\frac{\Delta T}{T}\ 100 = \frac{\lambda}{\ell}\ 100 = -\frac{\Delta B_z}{B_z}\ 100$$

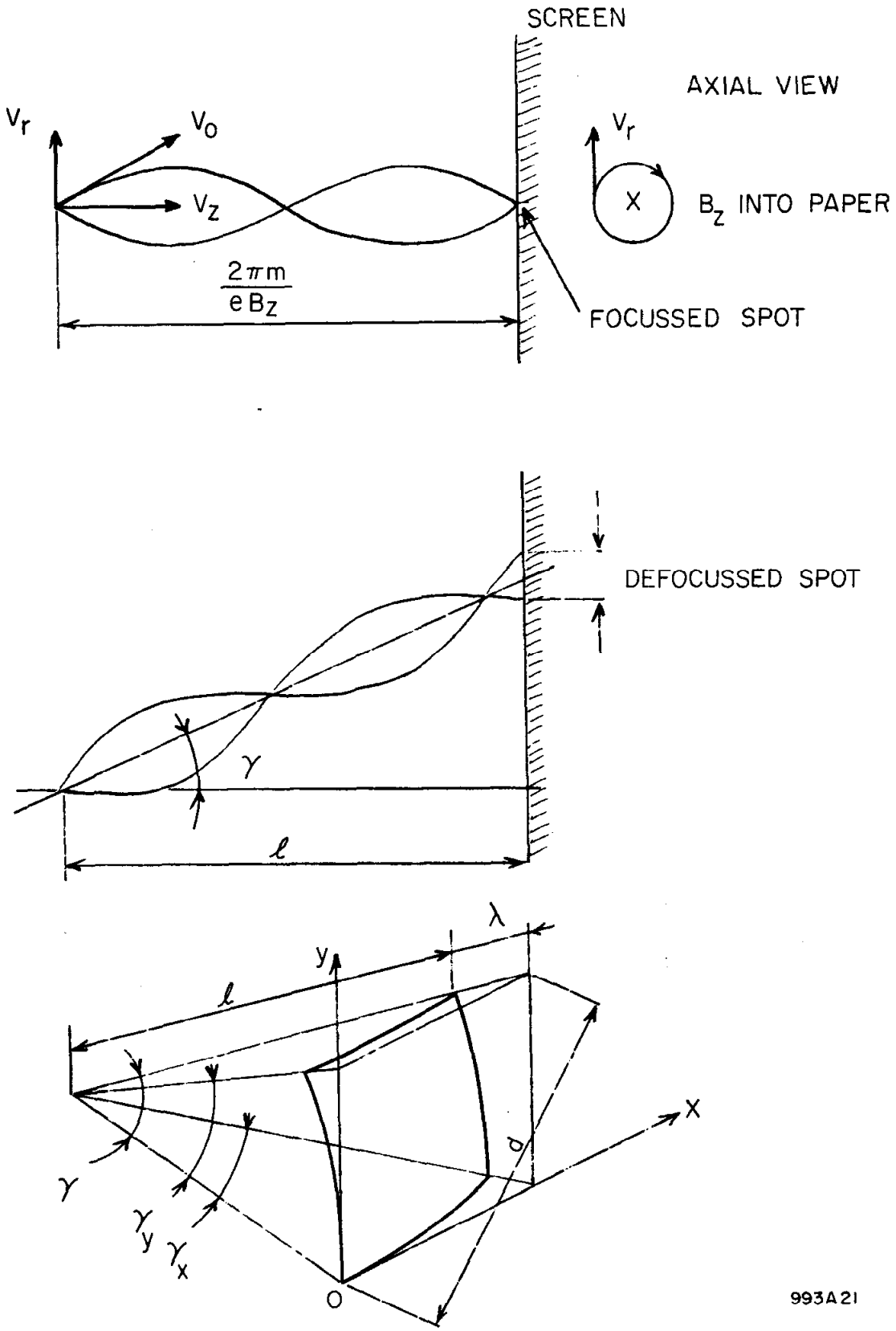

FIG. 19--Deflection defocusing.

With the help of Fig. 19, one gets:

$$\lambda = \frac{d}{\sin \gamma} - \ell = \ell \left[\frac{1}{\sqrt{1 - \sin^2 \gamma}} - 1 \right]$$

$$\lambda = \ell \left[\frac{1}{2} \sin^2 \gamma + \frac{3}{8} \sin^4 \gamma + \ldots \right] \tag{13}$$

for $\gamma = \pm 21^o$, one obtains:

$$- \frac{\Delta B_z}{B_z} \times 100 = \frac{\lambda}{\ell} \times 100 = 6.4\% + 0.6\% + \ldots \tag{14}$$

Assuming one would like to make ΔB_z vary as $\sin^2 \gamma$, the exact expression for $\sin^2 \gamma$ is:

$$\sin^2 \gamma = \frac{\sin^2 \gamma_x + \sin^2 \gamma_y - 2 \sin^2 \gamma_x \sin^2 \gamma_y}{1 - \sin^2 \gamma_x \sin^2 \gamma_y} \tag{15}$$

Since $\sin \gamma_x$ and $\sin \gamma_y$ are proportional to the x and y coil currents respectively, a good approximation for $\sin^2 \gamma$ is

$$\sin^2 \gamma \approx \Delta B_z \approx I_x^2 + I_y^2 \tag{16}$$

Indeed for $\gamma = \pm 21^o$

$$\gamma_x = \gamma_y = \pm 15^o$$

and $$- \frac{\Delta B_z}{B_z} \times 100 \approx \frac{1}{2} (\sin^2 \gamma_x + \sin^2 \gamma_y) \times 100 = 6.6\%.$$

A focus correction of the type indicated by Eq. (16) will refocus within 1%. For the H. B. I, variations in spot size of a few percent are hardly discernible, and it was found that a correction field of the form

$$\Delta B_z \approx |I_x| + |I_y| \tag{17a}$$

was still satisfactory. The function $|I_x| + |I_y|$ is generated according to Fig. 20(a) and used to control the dynamic focus coil current of H. B. I. The same circuit, modified by the introduction of a non-linear element in order to approach

$$\Delta B_z \approx I_x^2 + I_y^2 \tag{17b}$$

is applied to H. B. II. This correction function is a family of parabolas.

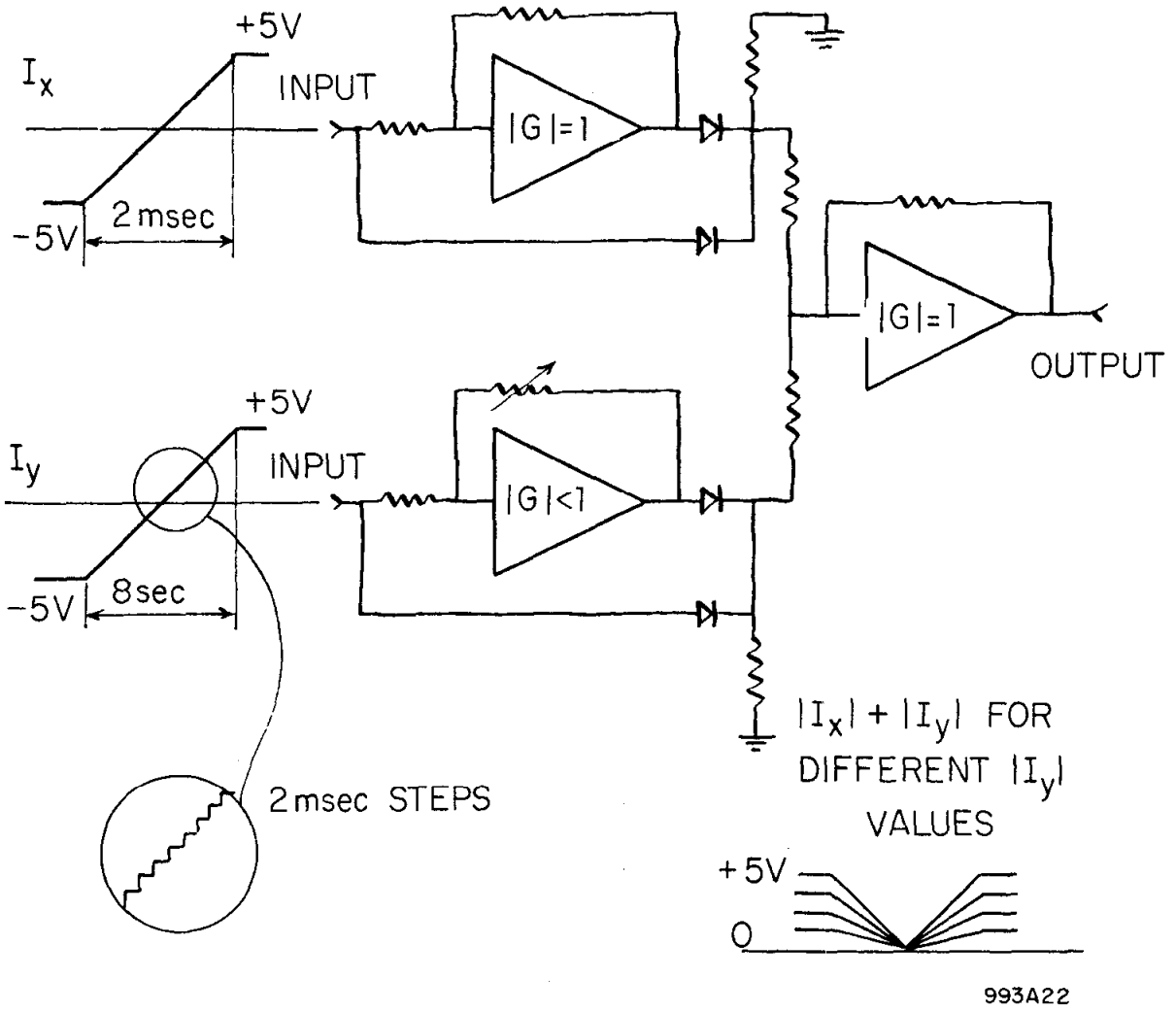

FIG. 20a--Dynamic focusing waveform generation.

Linear Sweep Generation. Figure 20(b) describes the integrator which generates the deflection and focus correction signal required for each scan line.

The operational amplifier used, has very little drift, (2 $\mu V/^{o}C$), and the feedback capacitor has a temperature coefficient of 70 PPM/^{o}C. The resetting of the integrator can be performed efficiently down to less than 0.5 MV, in 10 μsec, by using two field-effect transistors in parallel, to discharge the capacitor.

The sweep reproducibility has been measured to be of the order of 1 part in 20,000 at constant temperature.

Focusing Coils Data. Any combination of inductances are available for static and dynamic focusing coils. The units selected are shown in Table 3.

TABLE 3

Focusing Coils Data

Celco Number	HF 334-439/560	HF 334-439/700
Static coil inductance mH	40	40
Current Amp. at 27 kV	1	1
Dynamic coil inductance mH	0.25	0.01
Current Amp. dc at 27 kV	0.71	3.7
Current Amp. ac at 27 kV and at 30 kc/sec	1.35	7.1

A large inductance ratio between static and dynamic focusing coils has been selected which insures that fast changes in dynamic coil currents will not be interfered with by the static coil driving source impedance. In any case it is preferable to drive the static focus coil from a current source also. Both static and dynamic coils are therefore connected to sources analogous to the deflection amplifiers already described.

D. Spot Size and Pulse Detection

There is a large number of definitions for spot size, as well as a large number of methods used to measure it. It is not always clear what definition and what method are used in some manufacturers' specifications, and it is our opinion that the amount of modulation produced when scanning a particular grating is more useful as a criterion of spot effectiveness and as a means of comparing different tubes.

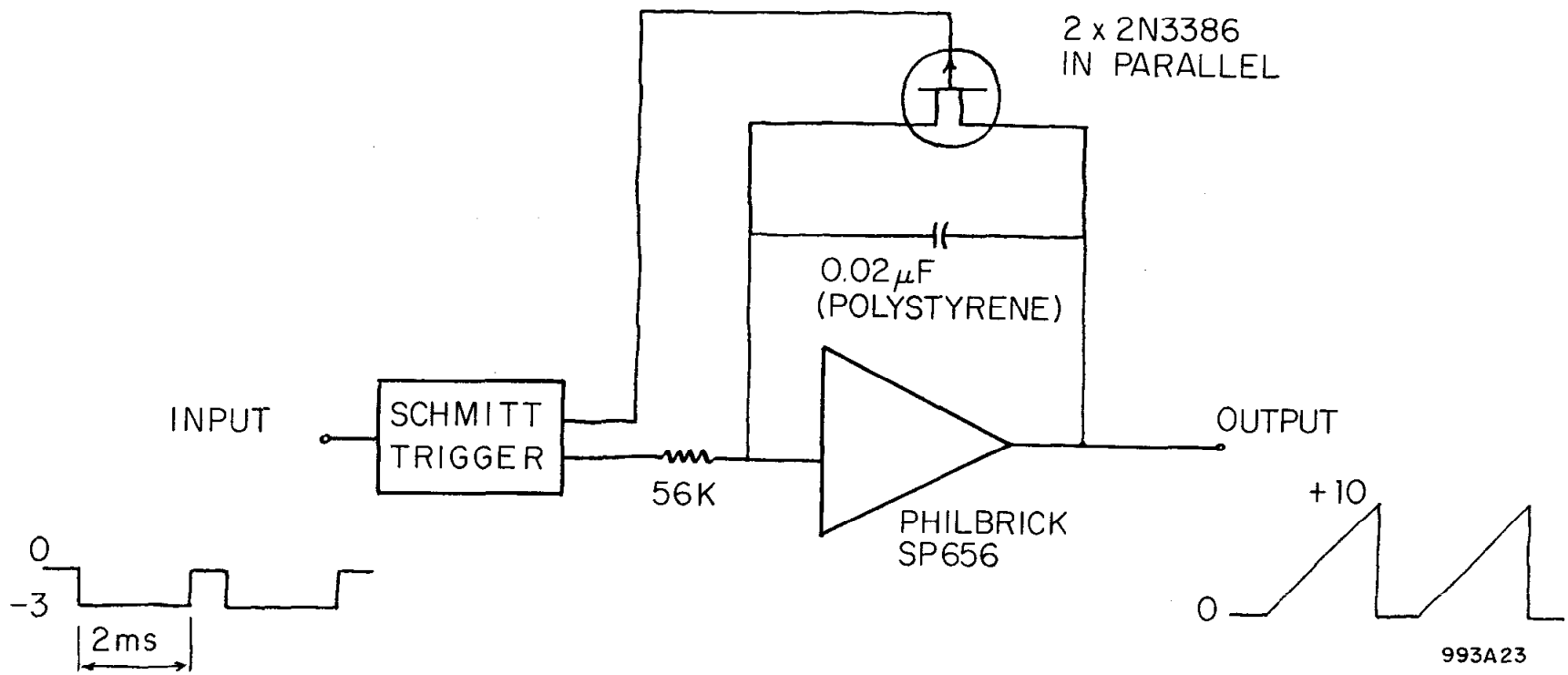

FIG. 20b--Generation of linear sweep.

We would like to analyze the mechanism of light modulation when a well-focused spot moves behind an opaque obstacle in the image plane. Due to the probabilistic character of light emission, the luminosity distribution is often assumed to be a Gaussian surface. Figure 21 shows such a surface and next to it, a parallelepiped which symbolizes the film data. We will assume that this data is completely opaque (Z dimension is very large) and is restricted in the x direction only.

Under these conditions the photomultiplier signal resulting from a linear sweep, will be proportional to the volume intercepted by the film obstacle

$$U(x) - U(x - x_0) \tag{18}$$

and the Gaussian surface

$$\frac{1}{\pi}\, e^{-(x^2+y^2)} \tag{19}$$

In other words the light modulation F(t) will be equal to the convolution of these two volumes in the x direction:

$$F(t) = \frac{1}{\pi}\int_{-\infty}^{+\infty} dy \int_{-\infty}^{+\infty} e^{-(x^2+y^2)} \left[U(t-x) - U(t-x-x_0)\right]\, dx \tag{20}$$

since $\int_{-\infty}^{+\infty} e^{-y^2}\, dy = \sqrt{\pi}$, we obtain:

$$F(t) = \frac{1}{\sqrt{\pi}}\left[\int_{-\infty}^{t} e^{-x^2}\, dx - \int_{-\infty}^{t-x_0} e^{-x^2}\, dx\right] \tag{21}$$

The integrals can be expressed in terms of the error function erf(t) and it complement erfc(t):

$$F(t) = \frac{1}{\sqrt{\pi}}\left[-\frac{\sqrt{\pi}}{2}\, \mathrm{erfc}(t) + \frac{\sqrt{\pi}}{2}\, \mathrm{erfc}(t - x_0)\right]$$

$$F(t) = \frac{1}{2}\left[+\mathrm{erf}(t) - \mathrm{erf}(t - x_0)\right] \tag{22}$$

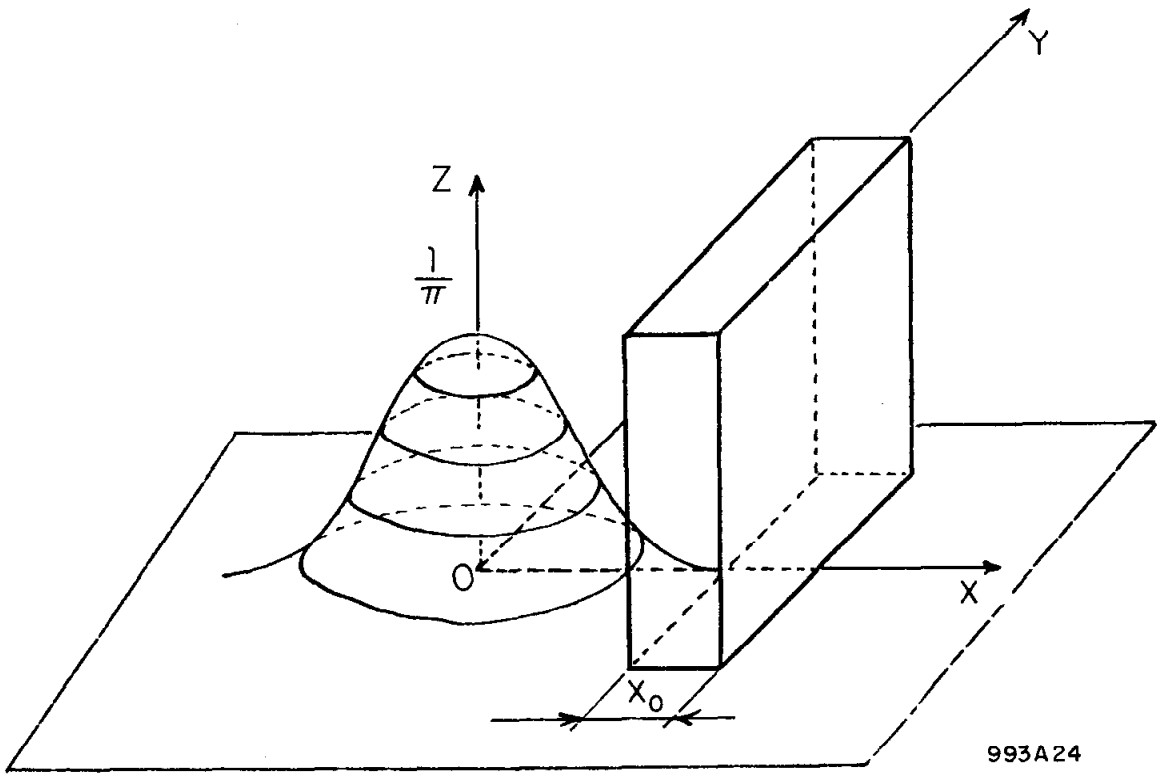

FIG. 21--Light spot sweeping over film data.

F(t) can now be determined graphically from plots of erf(t)[9] as indicated by Fig. 22.

For instance, assuming one wants to know the amount of modulation produced by scanning a 25-microns line, with a spot having a luminosity spread of 25 microns in the image plane, and moving at a speed of 18 microns/μsec. The functions of interest is of the form

$$e^{-\frac{2x^2}{(25)^2}} \qquad x \text{ in microns}$$

with $x_0 = 25$ microns. Figure 22 indicates the following results:

1. The maximum modulation is 67% only,
2. The width of F(t) at the $\frac{1}{\sqrt{2}}$ amplitude level, is equal to the luminosity spread,
3. To obtain 100% modulation, x_0 should be at least four times wider or 100 microns.

Signal to Noise Ratio. The photomultiplier signals of Fig. 23 indicate the presence of a fairly large amount of noise. Most of this noise is photomultiplier noise and its spectrum extends down to the kilocycle region. Filtering will improve slightly the signal to noise ratio, and we want to examine under what conditions this ratio can be maximized. Photomultiplier noise (shot noise) can be evaluated from:

$$\overline{i_n^2} = 2e\, I_0\, GB\, \frac{\delta}{\delta - 1} \tag{23}$$

i_n^2	mean square noise current
e	electron charge
I_0	anode average current
G	photomultiplier current gain
B	observation bandwidth
δ	individual dynode gain

The actual mode of operation is such that the output signal peak amplitude S_0 is equal to I_0. Therefore:

$$\frac{S_0}{N_0} = \frac{I_0}{\sqrt{\overline{i^2}}} = \sqrt{\frac{S_0}{2e\, GB\, \frac{\delta}{\delta - 1}}} = \text{Const.} \sqrt{\frac{S_0}{G}} \tag{24}$$

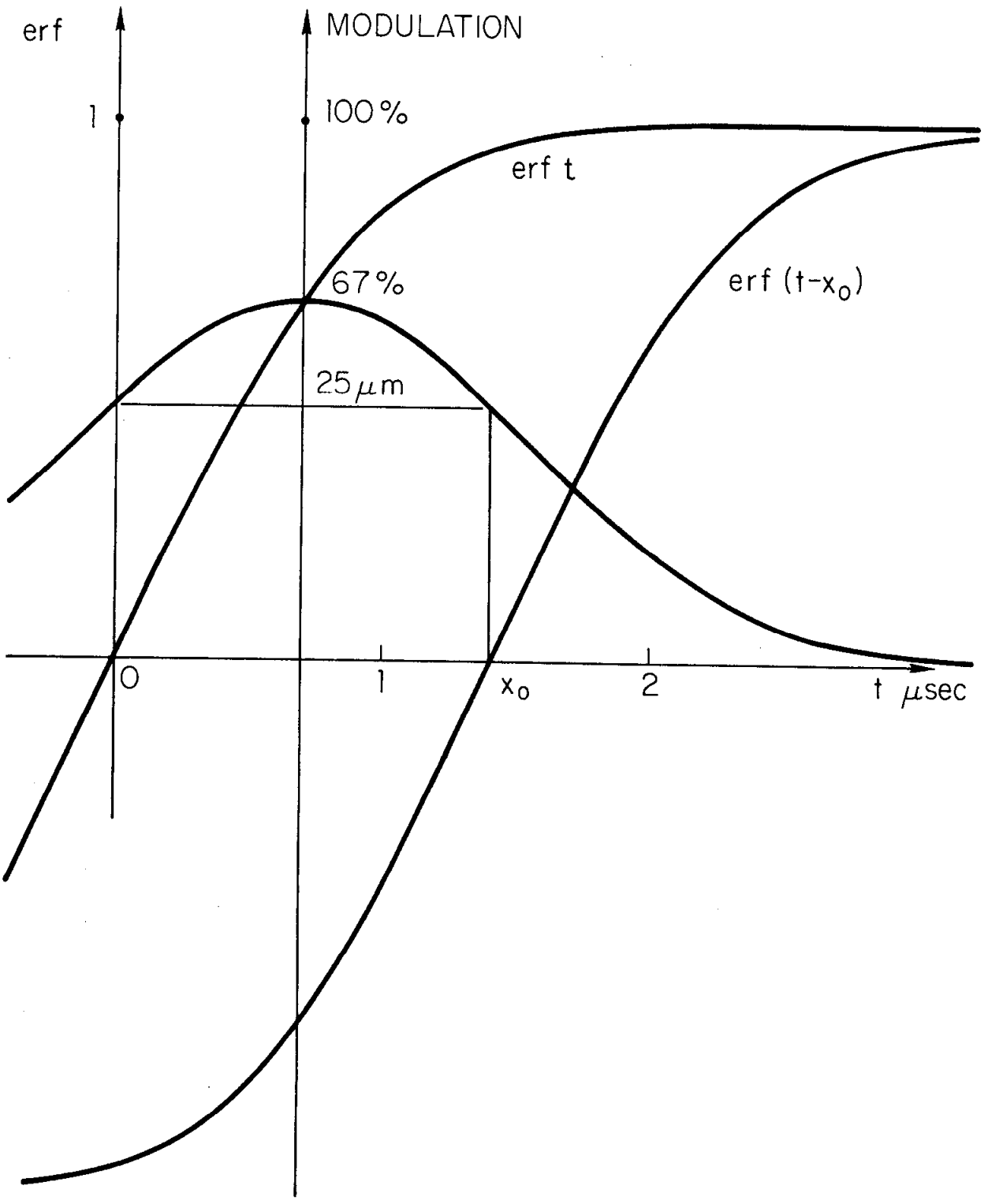

FIG. 22--Modulation from a 25 micron line with a luminosity spread of 25 microns and a sweep speed of 18 microns/μsec.

Top: Un-filtered photomultiplier signal 20 mV/cm

Bottom: Filtered and amplified photomultiplier signal 5 V/cm.

Time base: 0.2 ms/cm

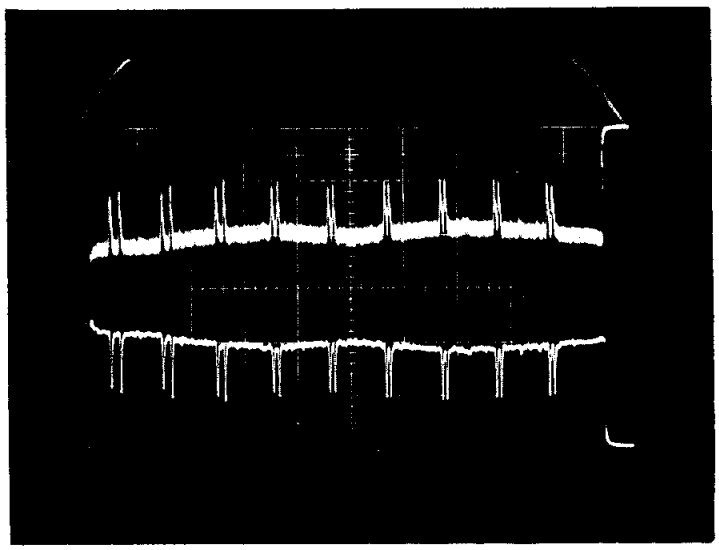

993A26

FIG. 23--Unfiltered and filtered photomultiplier signals.

This definition of signal to noise ratio is not the usual one, because a peak voltage ratio rather than a power ratio, is of interest here. This is somewhat improper, but what is meant by N_0 is: peak noise amplitude below the minimum usable threshold. Returning to relation (24), it is clear that S_0/G is the input signal or the peak spot luminosity. Therefore the output signal-to-noise ratio does not depend on the photomultiplier gain but is proportional to the square root of the luminosity. Thus high light output is very desirable.

S_0/N_0 can be calculated for some typical conditions:

PM tube Amperex 6810

$I_0 = S_0 = 2$ mA

$e = 1.6\ 10^{-19}$ Coulomb

$G = 10^6$

$B = 30$ Mc (oscilloscope bandwidth)

$\delta = 4$ (10 dynodes)

One obtains $S_0/N_0 = 12.5$. This is not very large.

Filtering will reduce considerably the output noise power but will not affect very much the peak noise exceeding the circuit threshold in the signal bandwidth.

E. Filtering and Track Center Circuits

From the results of Fig. 22 we expect pulses of the form $f(t) = e^{-\alpha t^2}$; if their spread is 25 microns or 1.4 μsec. α is found to be such that $1/\sqrt{\alpha} = 1$ μsec. The pulse frequency spectrum is given by the Fourier transform of f(t):

$$\left|F(\omega)\right| = \sqrt{\frac{\pi}{\alpha}}\ e^{-\frac{\omega^2}{4\alpha}} \qquad (25)$$

To preserve entirely the shape of f(t), a filter should have a large bandwidth and a linear phase. As a filter spectrum is made narrower, its response g(t) to f(t) becomes wider. For instance, a low pass filter with Gaussian amplitude and linear phase such as:

$$H(\omega) = H_0\ e^{-\frac{\omega^2}{4\alpha}}\ e^{j\omega t_0} \qquad (26)$$

will give a response:

$$g(t) = \text{inverse Fourier } \left[F(\omega) \cdot H(\omega)\right]$$

$$g(t) = H_0 \frac{1}{\sqrt{2}} e^{-\frac{\alpha}{2}(t - t_0)^2} \tag{27}$$

We see that the pulse shape is preserved but the spread is not 1.4 μsec anymore but 2 μsec. The time delay introduced is due to the phase factor and does not produce any distortions here.

The widening of the pulses and their delay is perfectly tolerable, but most of all their symmetry should not be altered if their center is to be determined accurately. Furthermore, it would be desirable that g(t) return quickly to the base line in order to intersect sharply with the threshold. This is not the case for the Gaussian filter which has an impulse response being a Gaussian function also.[10]

An "almost ideal" filter behaves in the opposite way. Indeed its impulse response is

$$h(t) = A \frac{\sin \omega_c t}{\omega_c t} \tag{28}$$

and the ringing of this function is quite troublesome. A compromise between these two types of circuits is a filter having an impulse response of the form:

$$h(t) = B \sin^2 \frac{t}{T} \tag{29}$$

In fact symmetry and absence of ringing can be obtained if the filter phase response is linear, i.e., the time delay is maximally flat. The synthesis of such networks has been extensively studied by W. E. Thomson.[11]

Figure 24 shows the amplitude response of the three different types of filters, all of them yielding the same half amplitude pulse width. The sine-squared filter is seen to track the Gaussian filter at low frequencies. Of course none of these two filters is as efficient as the "almost ideal" filter for noise rejection.

Figure 25 indicates the circuit of two filters and compares their impulse response. The advantages of the sine-squared filter are obvious.

Pulse Center Determination - Method Number 1. One philosophy of pulse center determination is outlined in Ref. 12. It consists in generating a pulse at the time a PM pulse intersects with itself when delayed by Δt. Indeed for

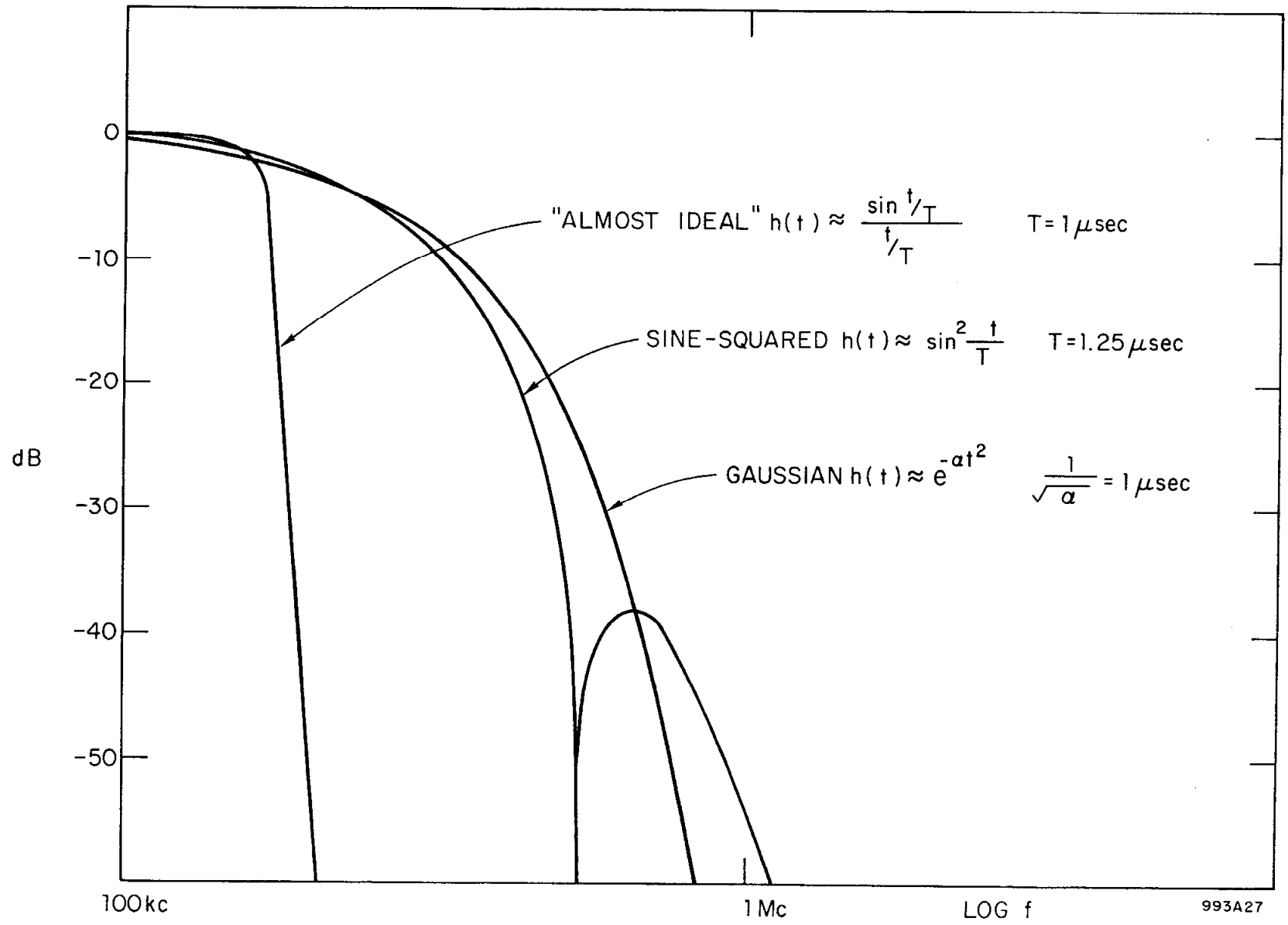

FIG. 24--Amplitude characteristic and impulse response of three filters yielding same half amplitude pulse width.

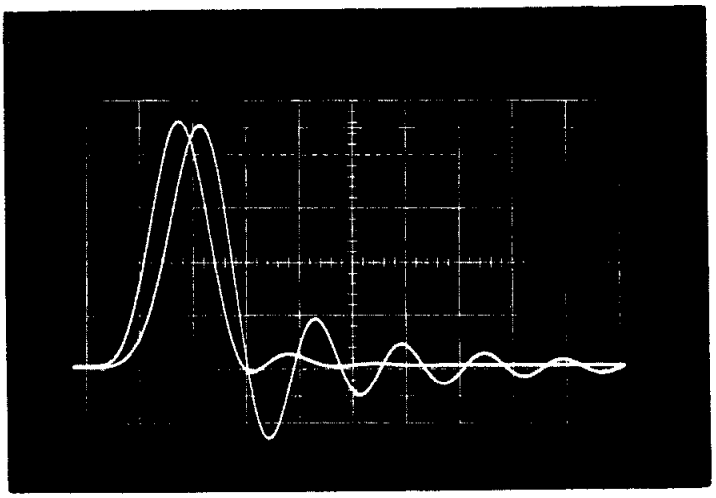

993A28

FIG. 25--Filter configurations.

Impulse response of $\frac{\sin \omega_c t}{\omega_c t}$ and $\sin^2 \frac{t}{T}$ filters

Input impulse area: 40 V μsec

Scales: 2 V/cm 2 μsec/cm

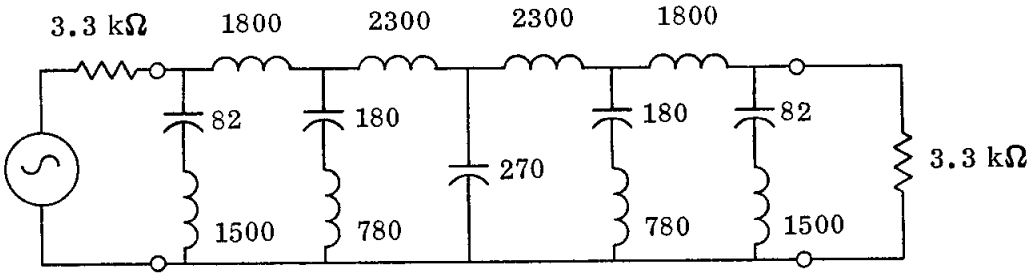

(a) $\frac{\sin \omega_c t}{\omega_c t}$ filter C's in pF L's in μH

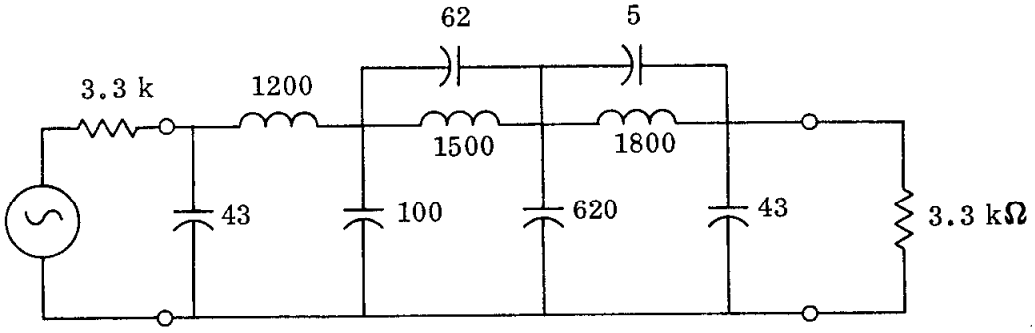

(b) $\sin^2 \frac{t}{T}$ filter C's in pF L's in μH

symmetrical pulses, the crossing will occur an amount of time $\Delta t/2$ after the effective pulse center, and all data will be shifted in time by the same amount (Fig. 26).

The circuit is very accurate for pulses of constant width, but when the size of the film obstacles vary widely, it requires different values of Δt. The crossing occurs with nearly zero slopes or at noise level.

Pulse Center Determination - Method Number 2. A direct sensing of the pulse center is achieved by detecting the time at which the pulse derivative becomes zero. This detection can be performed in a very reliable way by applying the differentiated pulse as a current input to a properly biased tunnel diode.

Since a differentiator output is proportional to frequency and is therefore very sensitive to noise, the differentiation range was strictly limited to the useful bandwidth by using a double-stop differentiator. Furthermore an amplitude discriminator provides a gate turning "on" or "off" the zero crossing detector output according to the desired threshold (Fig. 27).

The operation of the tunnel diode discriminator and zero crossing detector is described by Fig. 28. Note that for the selected threshold, one pulse only is permitted to cycle the diode characteristic, whereas both zero crossings are detected (Fig. 28, a and b respectively).

Figure 29 indicates the wave forms of interest.

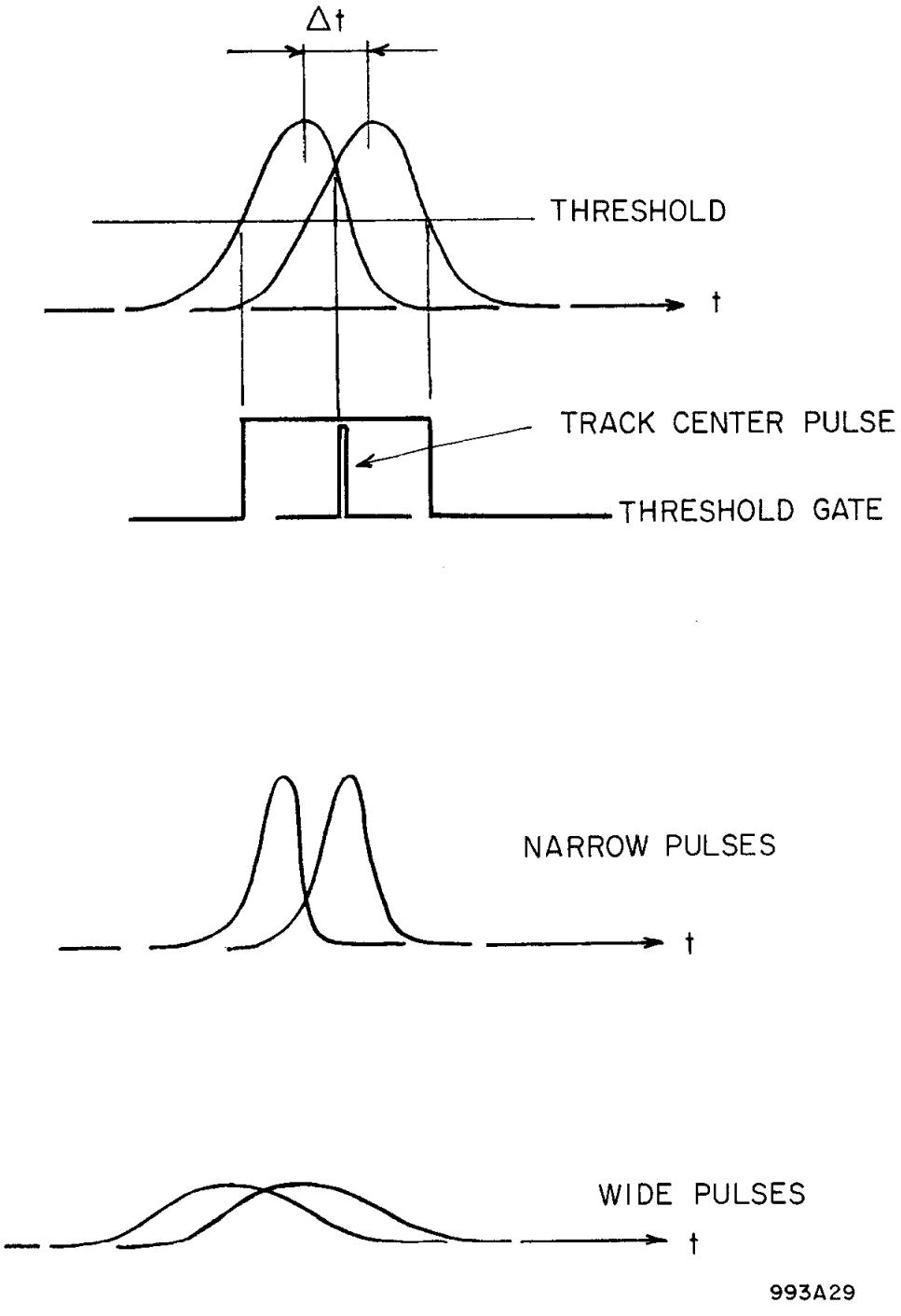

FIG. 26--Pulse center determination — Method No. 1.

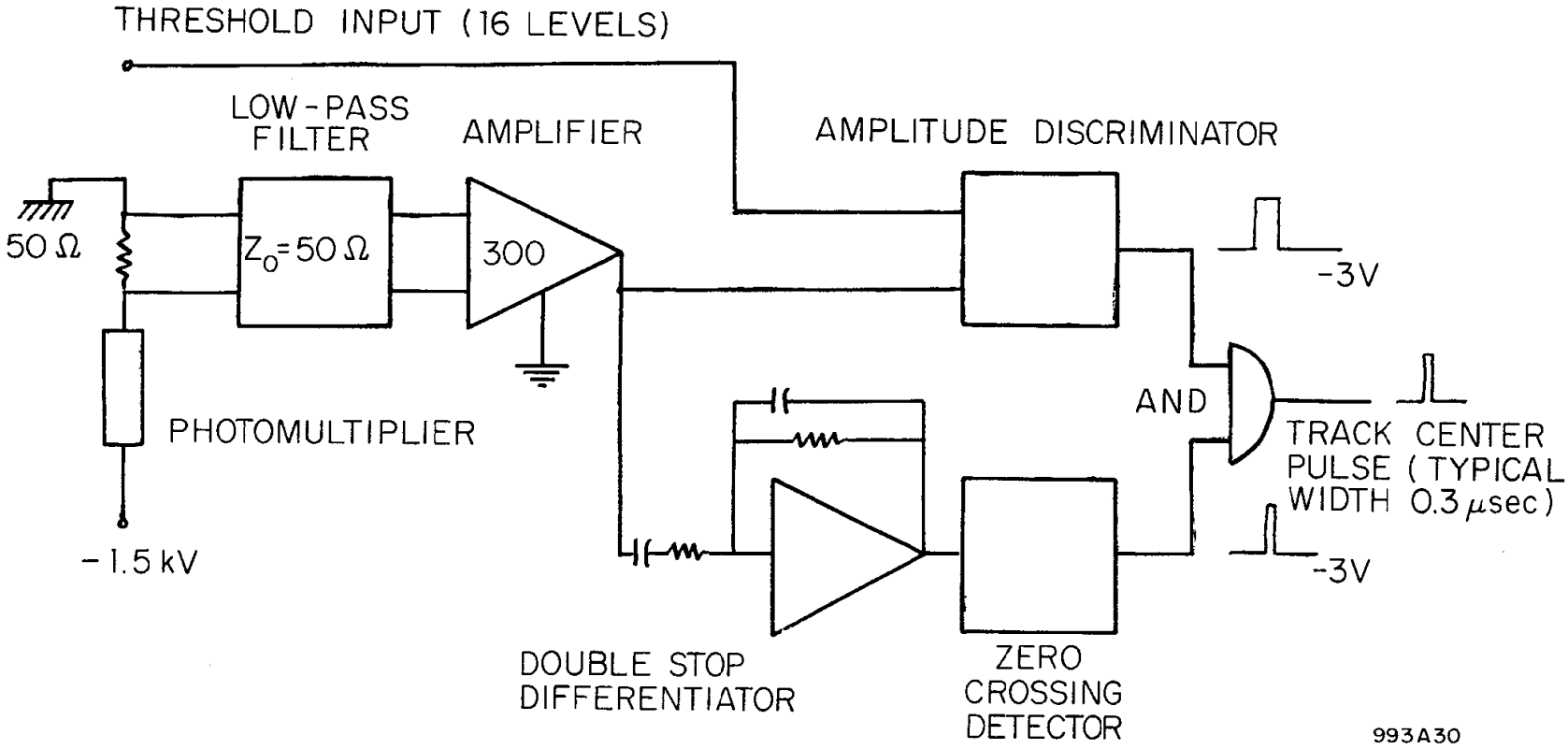

FIG. 27--Pulse center determination — Method No. 2.

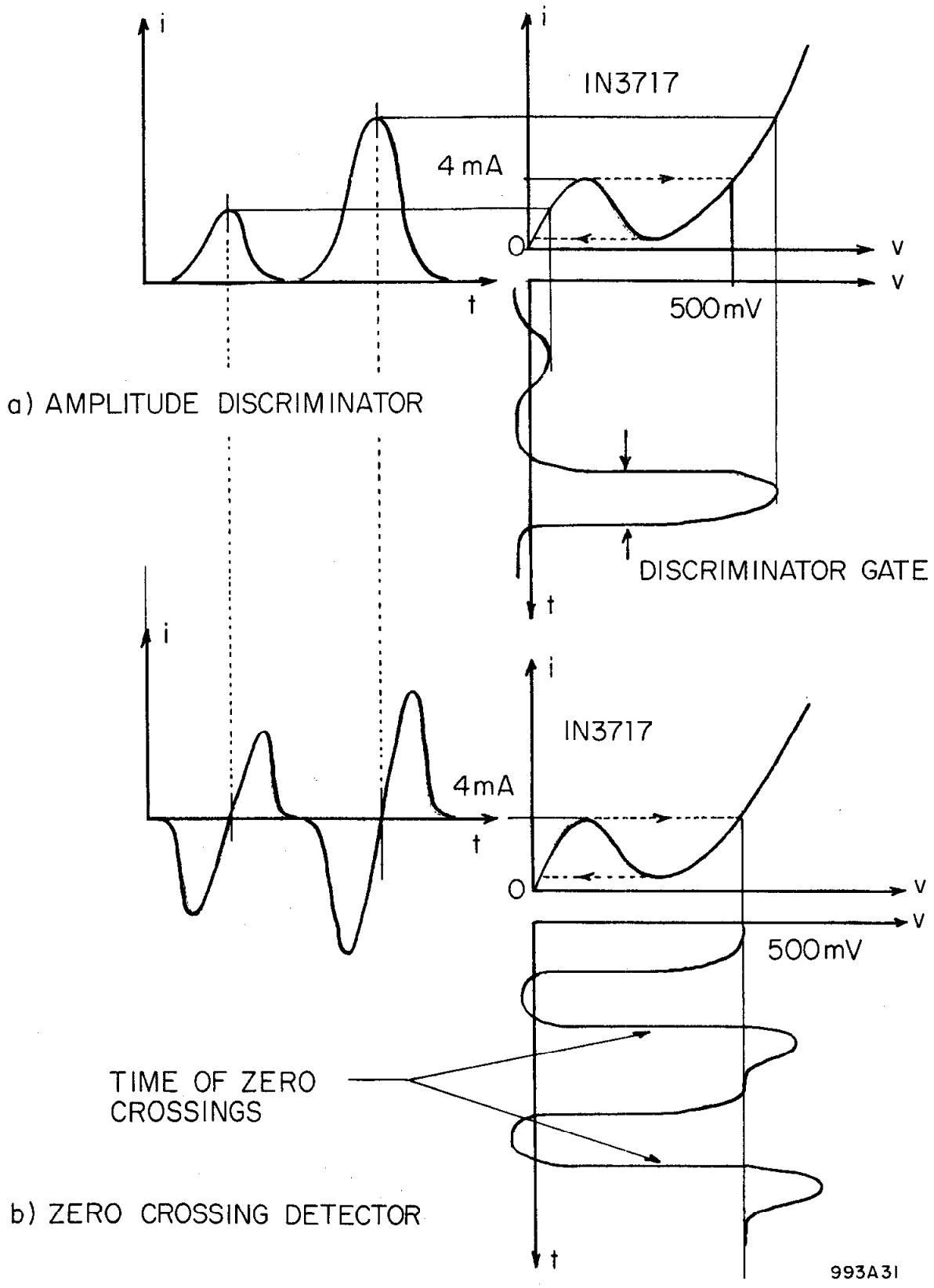

FIG. 28--Discriminator and zero-crossing detector.

Pulse and discriminator gate

2 V/cm 5 μsec/cm

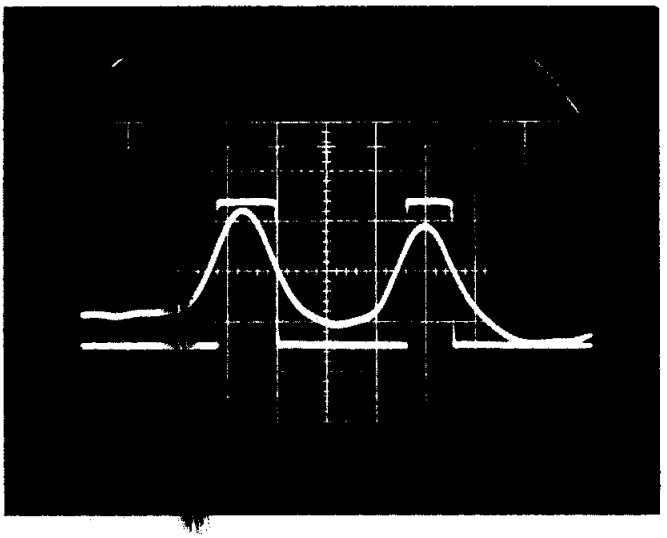

Differentiated pulse and zero detector output

2 V/cm 2 μsec/cm

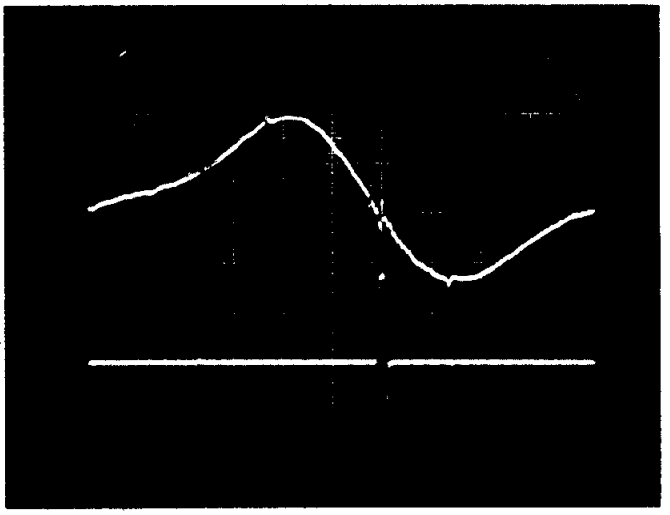

Photomultiplier pulse and its center

2 V/cm 2 μsec/cm

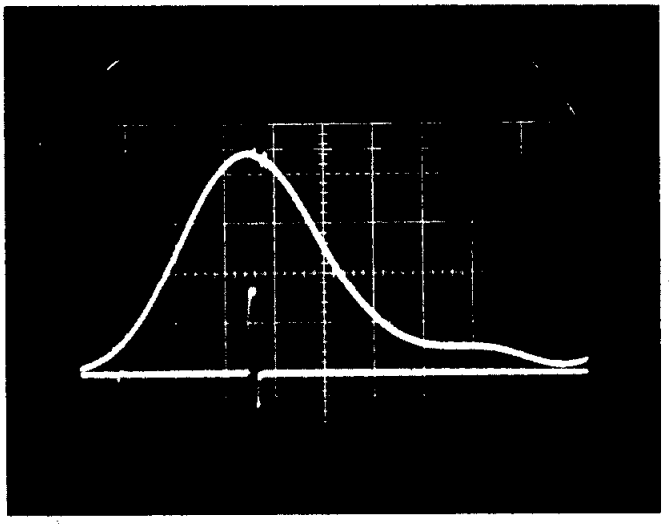

993A32

FIG. 29--Track center waveforms.

REFERENCES

1. R. P. Shutt, Editor, Bubble and Spark Chambers; Vol. II Principles and Use, (Academic Press, New York 1967); P.V.C. Hough, Chap. III, p. 141.
2. J. L. Brown, "Calibration of the Hummingbird Film Digitizer," SLAC Internal Note GSG, No. 5, Stanford Linear Accelerator Center, Stanford University, Stanford, California (April 1966).
3. IBM 2701 Data Adapter Unit, File No. S360-19, Form A 22-6844-1, International Business Machines, Systems Development Division, Kingston, New York (1966).
4. H. Slettenhaar, "Device Selector," Report No. SLAC-TN-67-33, Stanford Linear Accelerator Center, Stanford University, Stanford, California (1967).
5. H. Slettenhaar, "The Logic of the Hummingbird I and IX," Report No. SLAC-TN-67-34, Stanford Linear Accelerator Center, Stanford University, Stanford, California (1967).
6. H. Slettenhaar, "The Fast Logic of the Hummingbird II," Report No. SLAC-TN-67-35, Stanford Linear Accelerator Center, Stanford University, Stanford, California (1967).
7. J. van der Lans and V. Hamilton, "The Twenty-Two and a Half Display," Stanford Linear Accelerator Center, Stanford University, Stanford, California (in preparation).
8. J.-L. Pellegrin, "High Speed Deflection Amplifier for CRT Flying Spot Scanners," Report No. SLAC-TN-66-1, Stanford Linear Accelerater Center, Stanford University, Stanford, California (January 1966).
9. National Bureau of Standards, Handbook of Mathematical Functions with Formulas, Graphs, and Mathematical Tables, Milton Abramowitz and Irene A. Stegun, Editors, (Government Printing Office, Washington, D. C. 1965); 4th edition.
10. Athanasios Papoulis, The Fourier Integral and Its Applications, (McGraw Hill, New York 1962).
11. W. E. Thomson, "The Synthesis of a Network to Have a Sine-Squared Impulse Response," IRE Proc., Vol. 99 (1952); pp. 373-376.
12. J. van der Lans, "Pulse Midpoint Detector," Report No. BNL BCHP 03-7-A, Brookhaven National Laboratory, Upton, L. I., New York (1963) (U.S. Patent 3,345,575).